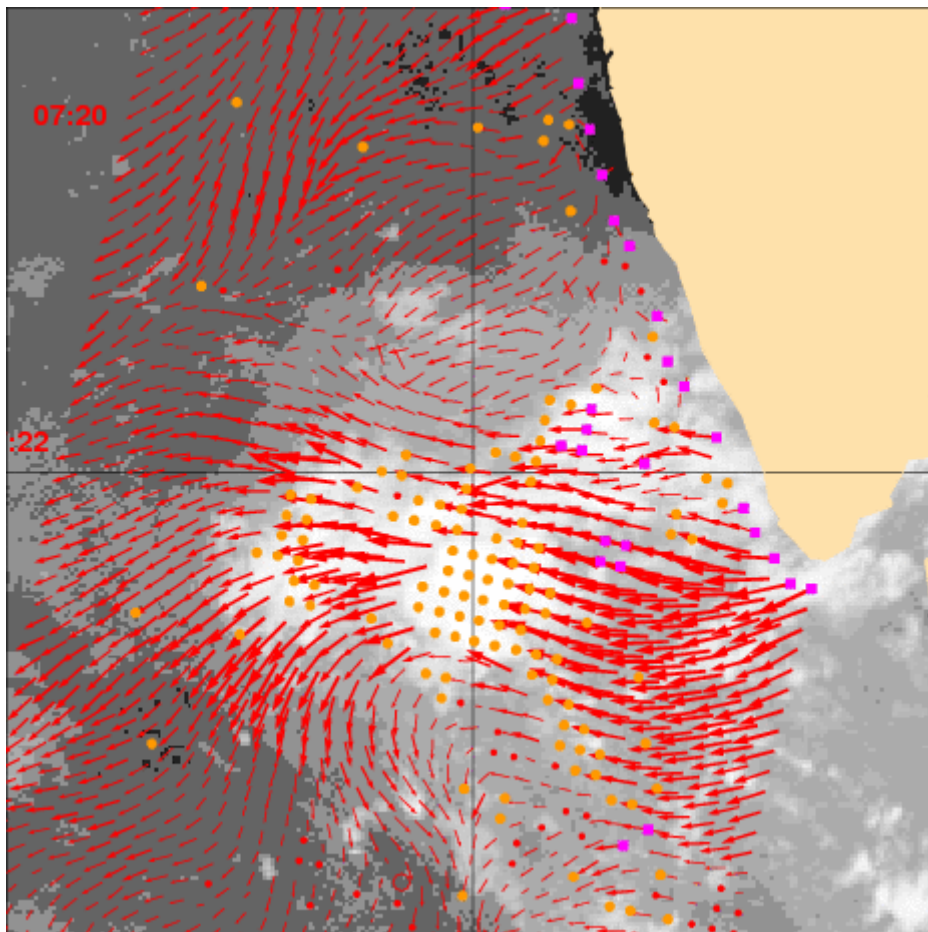


Research and Development in Europe on Global Application of the OceanSat-2 Scatterometer Winds

Final Report of OceanSat-2 Cal/Val AO project



NWPSAF-KN-TR-022

SAF/OSI/CDOP2/KNMI/TEC/RP/196

Authors:

Ad Stoffelen¹ (PI), Anton Verhoef¹,
Jeroen Verspeek¹, Jur Vogelzang¹, Gert-Jan Marseille¹, Tilly Driesenaar¹
Yun Risheng², Giovanna De Chiara³, Christophe Payan⁴, James Cotton⁵,
Abderrahim Bentamy⁶, and Marcos Portabella⁷

¹ KNMI, Royal Netherlands Meteorological Institute, de Bilt, the Netherlands

² MIRS, Chinese Academy of Sciences, Beijing, China

³ ECMWF, European Centre for Medium Range Weather Forecasts, Reading, United Kingdom

⁴ Meteo France, Toulouse, France

⁵ Met.Office, Exeter, United Kingdom

⁶ IFREMER, Institut Français de Recherche pour l'Exploitation de la Mer, Brest, France

⁷ CSIC, Barcelona, Spain

Final report of the project initiated in response to the Indian Space Research Organisation (ISRO) Announcement of Opportunity (AO) call for the calibration and validation of the OceanSat-2 mission instruments by the Royal Netherlands Meteorological Institute (KNMI) within the European Organisation for the Exploitation of Meteorological Satellites (EUMETSAT) Satellite Application Facility (SAF) Network under responsibility of the Numerical Weather Prediction (NWP) SAF and the Ocean and Sea Ice (OSI) SAF.

NWP SAF report number: NWPSAF-KN-TR-022

OSI SAF report number: SAF/OSI/CDOP2/KNMI/TEC/RP/196

27 May 2013

Contents

1.	Introduction	1
2.	Test data and processing method	3
3.	Evaluation of backscatter data	5
4.	Latitude-dependent correction	9
5.	NWP Ocean calibration	13
6.	NSCAT-3 GMF	17
7.	Evaluation of winds	19
7.1.	ECMWF model comparison	19
7.2.	Buoy comparison	21
7.3.	Triple collocation	26
7.4.	Future plans	27
8.	Applications	29
8.1.	Ocean Vector Wind Constellation	29
8.2.	Numerical Weather Prediction	29
8.3.	Other Applications	32
8.4.	Training	34
9.	Conclusions	35
	Acknowledgements	36
	References	37

1. Introduction

With great interest Europe welcomed the Indian Space Research Organisation (ISRO) scatterometer aboard OceanSat-2 (OSCAT), which favourably complements the METOP-A and MetOp-B Advanced Scatterometers (ASCAT), SeaWinds and the European Space Agency (ESA) European Remote-sensing Satellite (ERS-2) scatterometers. Recently, also the Chinese HY-2A scatterometer has been successfully launched, potentially part of a global constellation of scatterometers. Altogether, the meteorology and oceanography communities could expect to benefit of wind coverage at around 6, 10, 12, 18, 22 and 24 Local Solar Time (LST), which is proven useful for regional and coastal applications, but also for small-scale ocean forcing globally.

KNMI, in collaboration with the European Centre for Medium-Range Weather Forecasts (ECMWF), the Institut de Ciències del Mar (ICM – CSIC) in Barcelona, Spain, the French Research Institute for Exploitation of the Sea (IFREMER), Météo-France and the Met Office of the United Kingdom (UK), proposed to provide a European contribution on the following topics:

- Cal/Val, ocean calibration, validation of backscatter and wind data, including assessment of rain contamination;
- Weather and wave forecast impact assessment in global ECMWF and Météo-France, weather model and regional Aladin-Réunion models;
- Inclusion in the SAF global monitoring facilities of Near-Real Time (NRT) products;
- Synergetic use in global mesoscale L4 products, which in turn will be tested in ocean model forcing;
- Provision of a wind stress model, which has been accommodated through the provision of 10-m neutral winds and existing surface layer models; such as LKB;

These activities have been implemented by the proposing organizations, partly in the context of their contributions to the Satellite Application Facilities (SAFs) of the European organization for METeorological SATellites (EUMETSAT). An account of these activities is provided in this report.

Furthermore, a collaborative programme between ISRO and EUMETSAT has been set up through the EUMETSAT central facilities in liaison with NOAA, NASA and the EUMETSAT SAF network, much in line with the SAF scatterometer activities led by KNMI. The programme offered support to SAF visiting or associated scientists from either party, but no fitting activity has been set up to date. The incentive to carry out the proposed R&D work in collaboration with ISRO follows from the interest in a near-real time (NRT) distribution of OceanSat-2 scatterometer backscatter data, in line with World Meteorological Organization (WMO) resolution 40 (www.wmo.ch/pages/about/Resolution40_en.html). This would allow the use of the data in numerical weather prediction (NWP) by the proposing organisations, as part of their non commercial operational activities in support of protection of life and property. Much progress on the NRT availability of such data has been successfully achieved through renewed EUMETSAT-ISRO cooperation agreements and ISRO is greatly acknowledged for this.

The AO project has been restricted to R&D, in accordance with the terms of the AO and its objectives. However, the NRT access to OceanSat-2 scatterometer data has indeed significantly facilitated and sped up the “development of specific techniques for operational use of the data on a regional/ global basis” under the proposed project and thus also enhanced our feedback to ISRO.

The Oceansat-2 satellite was successfully launched in September 2009 by ISRO and level 2A (L2A) and level 2B (L2B) data were kindly provided to the Principle Investigator and ECMWF. The data have been evaluated in depth by the project team. Using the OSCAT Wind Data Processor (OWDP) software that was developed in the scope of the NWP SAF, KNMI produced L2B OSCAT winds as well. Moreover, this software allows on-the-fly Quality Assurance (QA) and Quality Control with well-established methods, which are essential for automatic application of the winds in numerical applications, such as NWP. Both the ISRO L2A backscatter data and the ISRO L2B and OWDP computed winds have been analysed, as further detailed in this report.

Due to popular demand and in agreement with ISRO policies the project has been extended from 2011 onwards to include additional non-commercial European users; all project participants are:

- EUMETSAT NWP and OSI SAF – KNMI (PI), Europe
- ECMWF - Europe
- IFREMER - France
- UK Met.Office - UK
- Meteo France - France
- ICM CSIC - Spain
- Instituto de Meteorologia - Portugal
- Fisheries and Sea Research Institute - Portugal
- Deutscher Wetterdienst - Germany
- University of Hamburg - Germany
- Norwegian Meteorological Institute - Norway
- Istituto di Scienze dell'Atmosfera e del Clima - Italy
- UTL-Technical University of Lisbon – Portugal

Since November 2012 many more European users access OWDP OSCAT winds due to EUMETCAST broadcasts. Moreover, international users now include among others:

- Japanese Meteorological Agency, JMA,
- Bureau of Meteorology, BoM,
- Environment Canada,
- Naval Research Lab. (USA),
- ENPE (Brazil),
- South Africa weather service,
- Hydrological and Meteorological Centre Russia, HMC
- German weather service, DWD
- Norwegian weather service, Met.No
- Portuguese weather service,
- Spanish weather service,
- Italian weather service,

It may be clear that wind data from India's OceanSat-2 scatterometer are a valuable resource in the international constellation of operational meteorological satellites. In particular, its local equator crossing time makes its data very complementary to other surface wind satellite data, allowing to depict processes such as the diurnal cycle, ocean interaction or atmospheric mesoscale convection. The NRT capability implemented by ISRO led to the first Indian satellite instrument data be operationally assimilated in several European NWP models, including ECMWF's. We look forward to the continuation of this successful mission.

2. Test data and processing method

The ocean normalised radar backscatter cross section is a geophysical quantity, i.e., independent of the instrument measuring it. The OSCAT Ku-band radar wavelength is almost identical to the NASA SeaWinds scatterometer radar wavelength. Therefore, the SeaWinds Geophysical Model Function (GMF) should be applicable to OSCAT as well. Moreover, the measurement configurations of SeaWinds and OSCAT are very similar, such that the scientific developments on the SeaWinds wind Data Processor (SDP) will be applicable for OSCAT. Since the NSCAT-2 GMF, covering a broad incidence angle range, is used in SDP, the modest incidence angle change from SeaWinds to OSCAT can be easily accounted for. The SDP winds have shown to provide superior buoy verification (Vogelzang et al., 2010). A first step to apply this processor is to map the OSCAT backscatter distribution onto the SeaWinds backscatter distribution, i.e., a calibration step. This step is also essential for a seamless extension of the SeaWinds wind climate data record to the OSCAT era and is described below.

The work described in this report is based on a test data set provided by ISRO from 2011 onwards. The data set contains L2A and L2B data in HDF5 (Padia, 2010) and covers the period of March 2011 to December 2012. The data have been created using ISRO processor version 1.3 (Attribute "Processor Version" in the HDF5 data files). The OSCAT Wind Data Processor (OWDP) was used to process the data and create L2B wind data in SeaWinds BUFR format (Leidner et al., 2000). The BUFR format is required by European users. OWDP uses the "genscat" software which contains general scatterometer data handling and wind processing routines that are also used by SDP, available through the NWP SAF (Vogelzang et al., 2010). OWDP is to a large extent based on SDP.

In the case of L2A HDF5 input data, OWDP averages the slice backscatter data to Wind Vector Cell (WVC) level:

$$\sigma^0 = \frac{\sum_s \alpha_s^{-1} \sigma_s^0}{\sum_s \alpha_s^{-1}}$$

where σ^0 is the WVC backscatter, σ_s^0 is the slice backscatter and α_s is the slice K_p -alpha. The weights α_s^{-1} were found to be proportional to the estimated transmitted power contained in a slice and thus the above weighting relates to a summation over backscattered power. The Sigma0 Quality Flag present in the HDF5 data is evaluated and slice data with one of the following flags set are skipped:

- Sigma0 is poor
- Kp is poor
- Invalid footprint
- Footprint contains saturated slice

These flags are only very rarely set in the L2A product, for example on 20 May 2012 the 'Sigma0 is poor' flag was only set in two slices and the other flags were never set. The WVC K_p values α , β and γ are computed from the slice K_p 's as

$$\alpha = \left(\sum_s \alpha_s^{-1} \right)^{-1}, \quad \beta = \left(\sum_s \beta_s^{-1} \right)^{-1}, \quad \gamma = \left(\sum_s \gamma_s^{-1} \right)^{-1},$$

the WVC received power P is computed from the slice received power as

$$P = \sum_s P_s, \quad P_s = 2 \cdot SNR_s / \beta_s$$

and the WVC SNR is calculated as

$$SNR = \beta \cdot P / 2.$$

Now $K_p^2 = \alpha + \beta / SNR + \gamma / SNR^2$ is obtained for each WVC view.

ECMWF NWP model sea surface temperature and land-sea mask data are used to provide information about possible ice or land presence in the WVCs. WVCs with a sea surface temperature below 272.16 K (-1.0 °C) are assumed to be covered with ice and no wind information is calculated. Land presence within each WVC is determined by using the land-sea mask available from ECMWF. The weighted mean value of the land fractions of all model grid points within 80 km of the WVC centre is calculated. The weight of each grid point scales with $1/r^2$, where r is the distance between the WVC centre and the model grid point. If this mean land fraction value exceeds a threshold of 0.02, no wind retrieval is performed.

Subsequently, OWDP inverts the WVC backscatter data to ambiguous wind solutions using the NSCAT-3 Geophysical Model Function (GMF). Earlier on in the project the NSCAT-2 GMF has been used, but it was found biased high at high winds. Winds in the outer parts of the swath, where only VV-polarised outer beam data are available at WVC numbers 1-4 and 33-36, have been computed by segregating the fore and aft measurements in two values, such that 4 backscatter values remain available in each WVC, which benefits the wind retrieval.

KNMI has put great effort in the QC of Ku-band pencil-beam scatterometer data and were the first to publish effective methods for screening of rain-contaminated WVCs. A basic quality control step is done after the wind inversion; all WVCs in which the wind solution closest to the NWP background wind has a Maximum Likelihood Estimator (MLE) value above a certain threshold are rejected. This procedure has been carefully tuned for SeaWinds and proves very effective for rain decontamination (Portabella and Stoffelen, 2001, 2002a,b). The OSCAT threshold is set such that the procedure rejects approximately 5% of the WVCs, a rejection rate which is the same as obtained in SDP for the SeaWinds data. Buoy verification has demonstrated the effective QC in SDP with respect to other SeaWinds wind products (Stoffelen et al., 2010).

Another important innovation of SDP is the application of a 2D variational meteorological analysis method, called 2D-Var, in combination with the Multiple Solution Scheme (MSS), where 144 wind solutions with their associated probabilities are considered (see Vogelzang et al., 2010). It addresses the problem that for a conically scanning pencil-beam scatterometer, wind speed and wind direction sensitivity are rather variable. This makes the wind retrieval process non-linear and therefore any local-minimum wind vector ambiguities non-optimal (Stoffelen and Portabella, 2006). The main purpose of MSS is to take full account of the local wind probability information as contained in the backscatter measurements and derived in the wind retrieval procedure (Portabella and Stoffelen, 2004). ECMWF model forecast (3 to 18 hours) winds are used to initialise the ambiguity removal step and ambiguity removal is performed in order to select the appropriate wind solution from the available options.

In the case of comparison to the ISRO L2B HDF5 input data; our analysis uses the ISRO-selected winds (Wind_speed_selection, Wind_direction_selection) rather than the ISRO ambiguities (Wind_speed, Wind_direction, WVC_selection) from the input. The former winds compare slightly better to the ECMWF model winds. The backscatter data in the constructed ISRO L2B BUFR output are missing in this case.

3. Evaluation of backscatter data

As a first step, the slice backscatter data present in the HDF5 L2A files have been evaluated. Figure 1 shows a plot of the slice KpA (a_s) versus the slice Sigma0 (σ_s^0). Since a_s depends on the slice bandwidth and on the transmit pulse width only (see section 5.1 in Padia, 2010), the distinct levels in the plot must correspond to different slice types in the egg footprint. Similar plots were made for β_s (middle pane of Figure 1) and γ_s (not shown here). Whereas processed version 1.2 at ISRO did not show low σ_s^0 values below approximately -50 dB for slices corresponding to high a_s or β_s values, such values do appear in version 1.3.

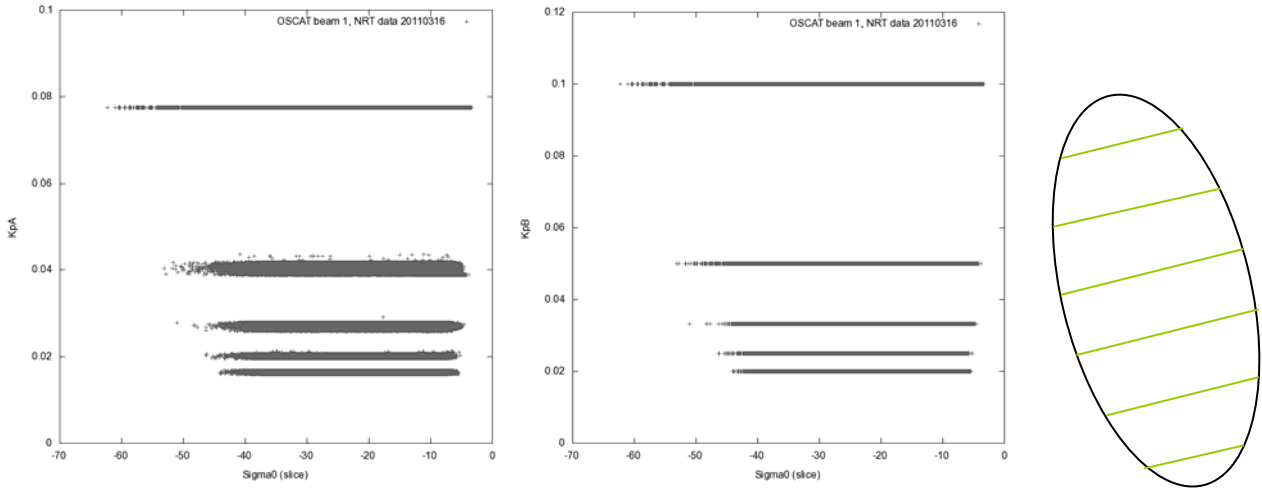


Figure 1: slice KpA versus slice Sigma0 (left), slice KpB versus slice Sigma0 (middle) and schematic drawing of slices forming an "egg" (right).

As a next step, we plotted collocated σ_s^0 values corresponding to the same WVC, but with different values of a_s , i.e. originating from different parts of the egg footprint, see Figure 2. This plot is made for the inner forward beam (HH), but the other beams show similar results. Since the backscatter data are from (almost) the same location on the Earth, a linear relation between the data along both axes is to be expected. However, in the scatter plot (left in Figure 2) it looks as if the σ_s^0 from different slice types are biased with respect to each other, especially for low backscatter values. This bias does not appear however when we plot the same slice backscatter values in a contoured histogram (right in Figure 2). There is no bias as can be seen from the red curve in the bottom right pane.

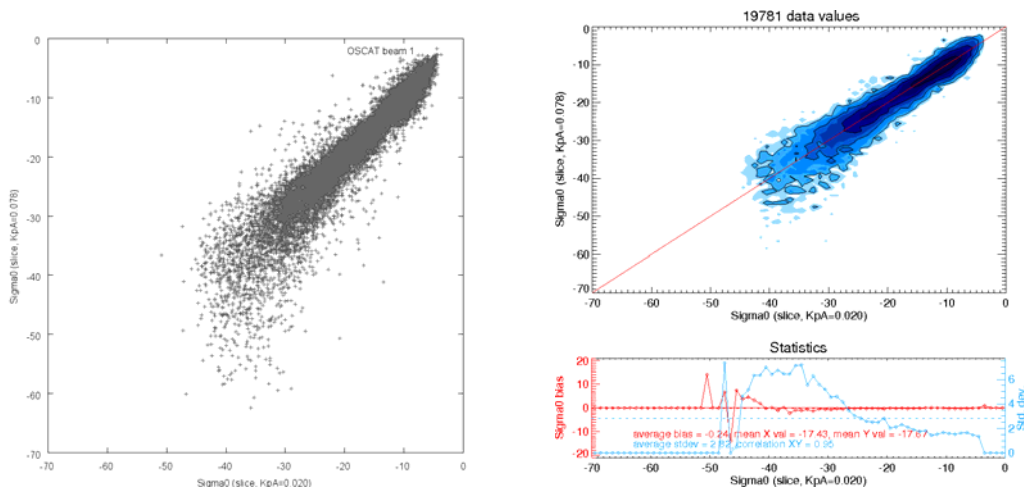


Figure 2: Scatter plot of slice Sigma0 corresponding to KpA of 0.078 versus slice Sigma0 corresponding to KpA of 0.020 (left) and the same plotted as contoured histogram.

The behaviour of the slice backscatter values around zero is shown in more detail in Figure 3 for version 1.2, where probability density functions (PDFs) of the σ^0_s are shown on differently binned horizontal scales. The left hand side plot shows an increasing distribution towards zero, followed by a decrease below 0.002. The decreasing trend is clearer in the right hand side plot. This is all to be expected, but two phenomena are striking: the dip in the distribution very close to zero and the fact that the distribution extends to negative values up to -0.005 and lower. The distribution for backscatter data corresponding to a KpA of 0.078 (not shown) show similar behaviour, except for the dip around zero which is replaced by a peak. From the PDFs we conclude that there may be an issue with the level 0 to level 1 processing for low σ^0_s values in ISRO version 1.2. This indeed has been corrected in version 1.3.

Figure 4 shows the PDF of the WVC σ^0 values as computed by OWDP. The results of the slice backscatter analysis are confirmed and it is clear that version 1.2 shows a cut-off below -40 dB which will influence the wind inversion results, especially in low wind regions.

In order to assess the quality of the instrument backscatter measurements, we computed expected WVC σ^0 values from the ECMWF model winds. The NSCAT2 GMF, used successfully in SDP for wind retrieval, was applied to the collocated model winds. Along the vertical axis we should thus expect the projected uncertainties due to ECMWF wind vector error and GMF. The simulated backscatter data are plotted against the measured WVC σ^0 values in Figure 5. The measured backscatter data (horizontal) contain measurement noise, here presented in dBs. Given the uncertainties and their transformation in dB, we evaluated the medians of the joint distribution. It is clear from the left plot that the median of the contour is not along the diagonal for lower backscatter values for version 1.2. In order to correct for this we applied a simple linear σ^0 correction below -27 dB. This results in a better linear relationship between expected and measured σ^0 , but the PDF is now cut off at even higher backscatter values of approximately -35 dB in version 1.2. Note that in the averaging process for the computation of the WVC backscatter values, the "Negative Sigma0" flag in the slice Sigma0 Quality Flag information was neglected, i.e., all slice σ^0 values are considered to be positive. When this flag is taken into account, in many cases negative σ^0 values occur on WVC level leading to a high fraction of WVCs where no winds can be computed. This is consistent with the results shown in Figure 3 in the previous section. These artefacts have been taken out in version 1.3 by an improved backscatter processing at low values. The bottom panel of Figure 5 shows that a simple correction of -0.65 dB provides a diagonal fit of the median backscatter values. This moves the low backscatter cut-off to -37 dB.

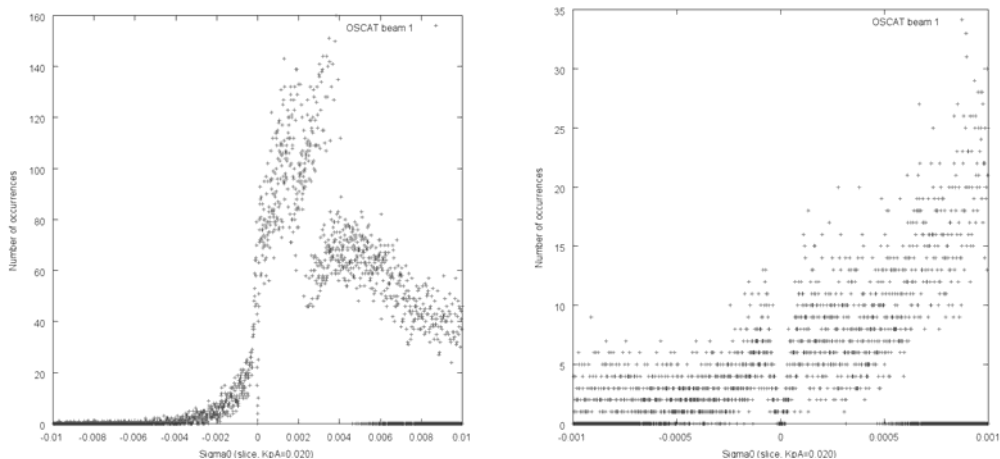


Figure 3: probability density function of slice backscatter values corresponding to slice KpA of 0.020 around zero. The scatter plots show the number of occurrences versus the slice Sigma0 on a coarse (left) and finer (right) scale. A Sigma0 of 0.01 corresponds to -20 dB, a Sigma0 of 0.0005 to -33 dB.

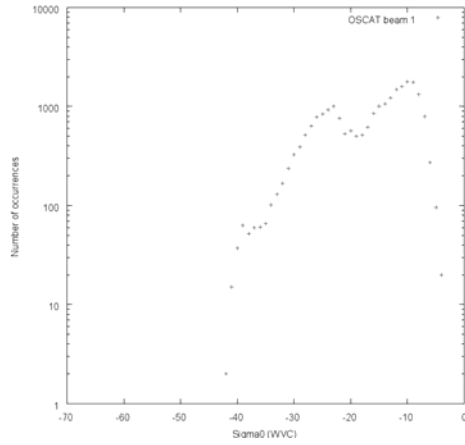


Figure 4: probability density function of WVC backscatter values. The Sigma0's are on a dB scale.

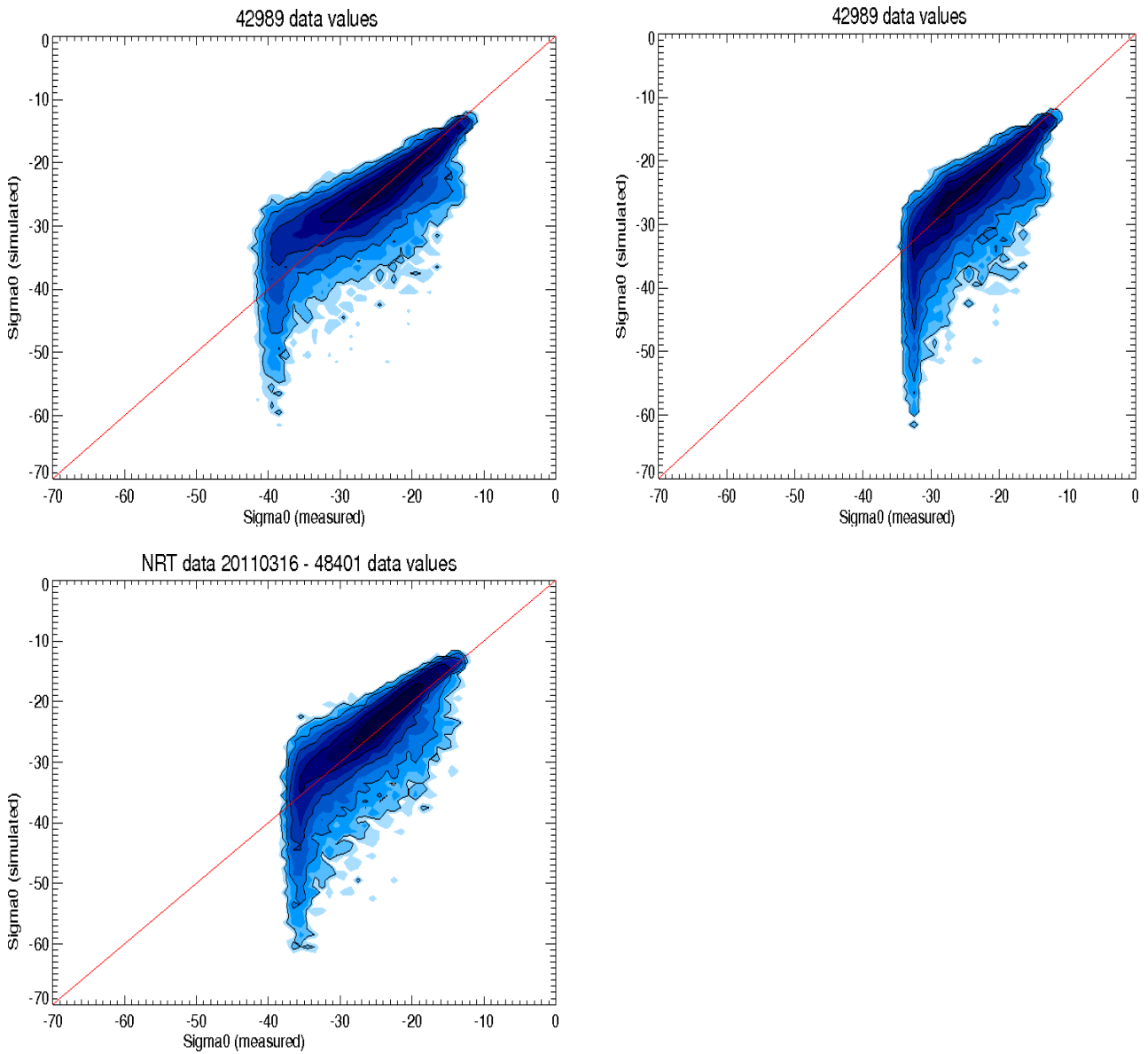


Figure 5: Contour plots of simulated WVC backscatter against measured WVC backscatter for the inner forward beam (HH), without (top left) and with (top right) σ^0 correction (see text) for version 1.2. The bottom plot is for version 1.3 and not corrected.

After this fit, WVC-dependent biases remain and therefore an additional bias correction was tried by applying an additional satellite height correction.

4. Latitude-dependent correction

Several users report negative biases of OSCAT winds with respect to Numerical Weather Prediction models in the southern hemisphere, notably for latitudes below -50° (Jelenak et al., 2012; Payan et al., 2012; De Chiara et al., 2012); see the example plot below.

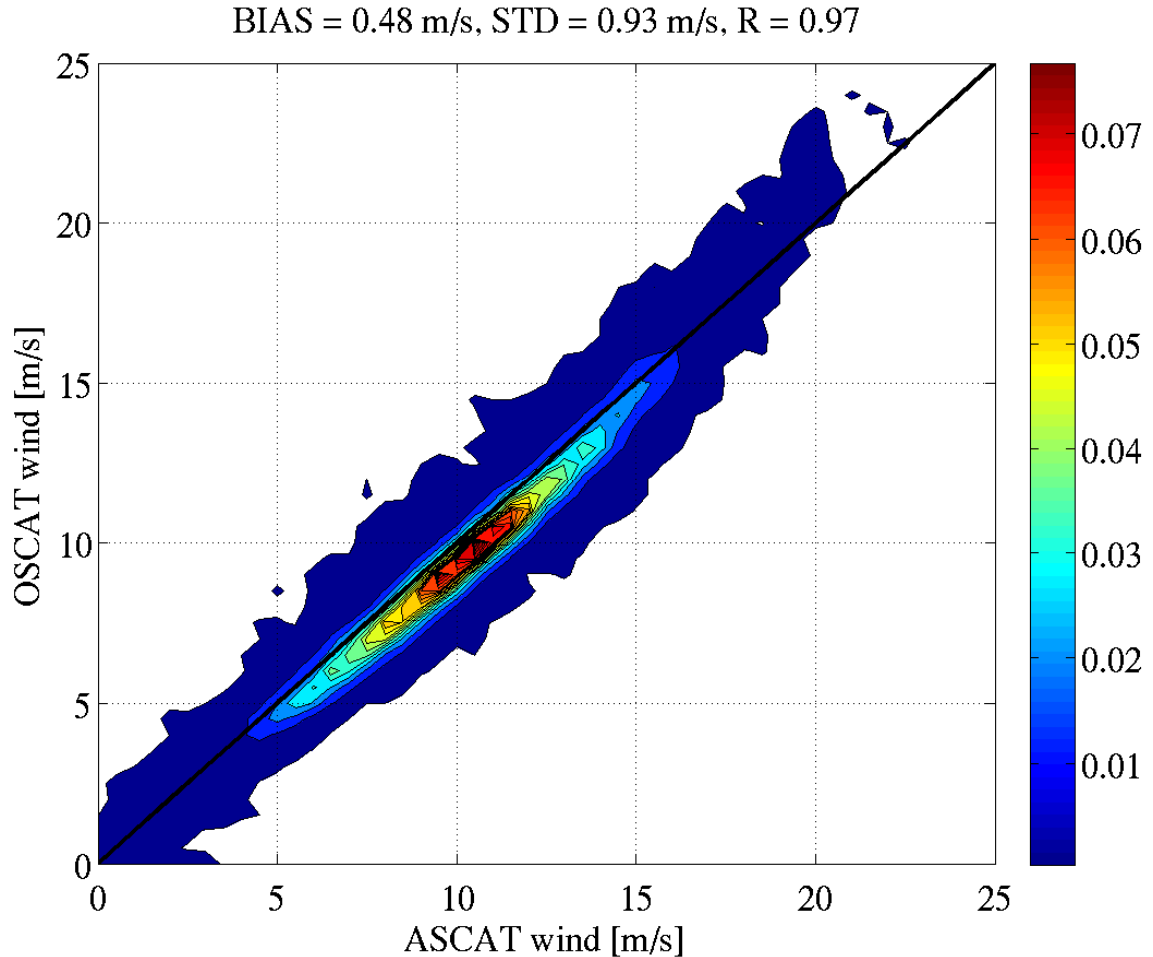


Figure 6: Collocated OSCAT and ASCAT winds in the southern hemisphere between 45S and 60S. Note the bias of around 1 m/s.

Following an inventory of potential causes, we have investigated if this can be related to the eccentric orbit of Oceansat-2, which has a higher altitude over the southern hemisphere than over the northern hemisphere. All plots in this document are from file S1L1B2012040_12598_12599.h5, but other files show similar results.

Although mean calibration differences between scatterometers, notably QuikScat and OSCAT, exist as well [6,7], these are not the focus of this note.

We expect that the correction for orbit height is applied in the X factor, which is related to the normalised backscatter σ_0 by $\sigma_0 = P_b / X$, where P_b is the backscattered radiation power. So over the southern hemisphere we expect lower values for X . The plots in Figure 7 show quite large variations of X , (associated with other dependencies of X) but also a clear latitude-dependent trend towards lower values in the southern hemisphere along rows of measurement points of about 0.35 dB.

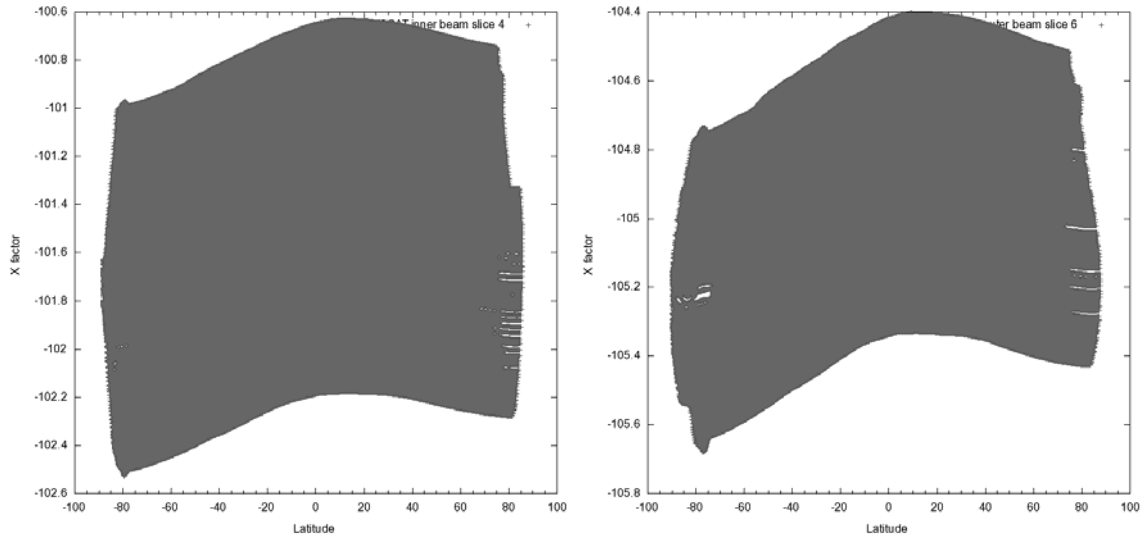


Figure 7: variation of X factor as a function of latitude for inner HH beam slice 4 (left) and outer VV beam slice 6 (right).

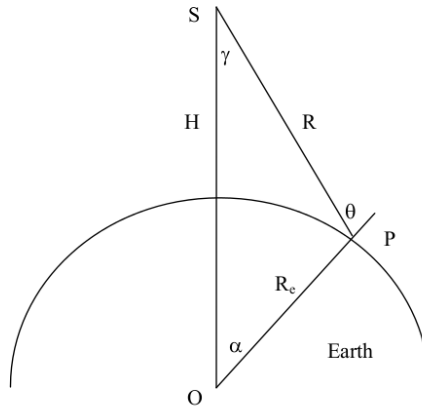


Figure 8: Definition of angles and radii (figure 5.3 from Padia (2010))

Now we will compute the expected height corrections for the backscatter from the orbit information as present in the level 1b data. The slant range R as a function of latitude can be computed from the orbit parameters (see Figure 8 for the definition of the angles and radii).

$\text{lat} = \sin^{-1}(p_z / (R_1 + 720))$, with p_z satellite orbit z -position and R_1 the Earth mean radius (6371.0 km; see Wikipedia, 2013). The orbit height is assumed to be 720 km. The distance to the Earth centre $H = \sqrt{p_x^2 + p_y^2 + p_z^2}$, where p_x, p_y and p_z are the satellite orbit positions. R_e (Earth radius for a given latitude) is computed using the formula in (Wikipedia, 2013) using the equatorial and polar Earth radii of resp. 6,378.1370 km and 6,356.7523 km.

The incidence angle $\theta = \sin^{-1}(\sin(\gamma)H / R_e)$, where γ is the beam look angle with respect to the sub-satellite point, 42.66° for the inner HH beam and 49.33° for the outer VV beam. The angle α between R_e and H is computed (knowing that the sum of angles in a triangle is 180°) as $\alpha = \theta + \gamma$.

Now the slant range R can be computed as $R = R_e \sin(\alpha) / \sin(\gamma)$, it is plotted for the HH and VV beams in Figure 9.

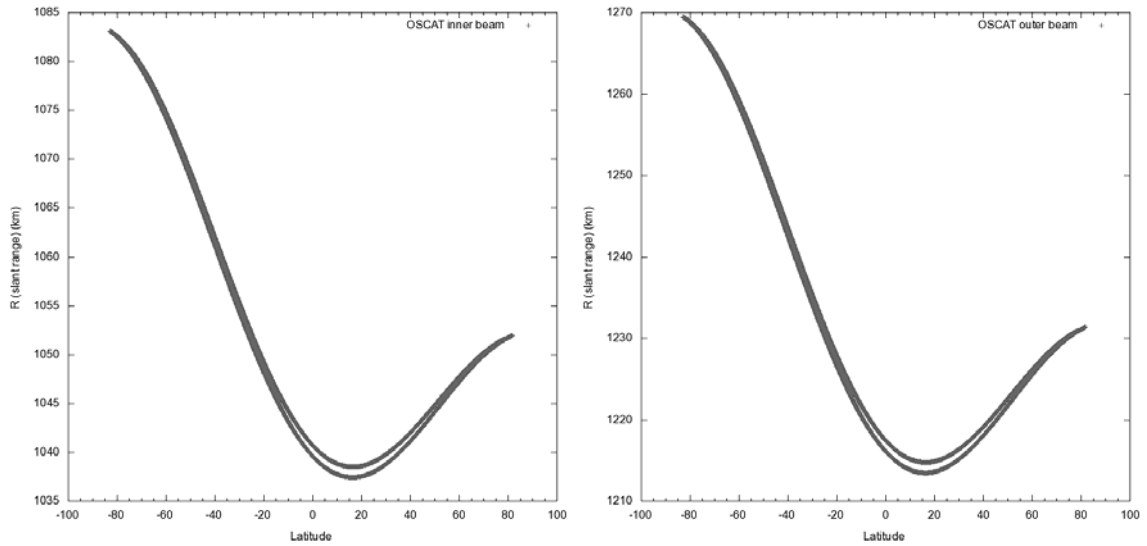


Figure 9: variation of slant range R as a function of latitude for inner HH beam (left) and outer VV beam.

Assuming that the received power by the radar instrument scales with $1/R^4$, we can compute the attenuation correction C_R in dB resulting from the variation in slant range using $C_R = 10 \cdot \log((R/R_{ref})^4)$ where the R_{ref} is an arbitrary reference height. A different value of R_{ref} will result in a vertical shift of C_R but it will not change the shape of the curve of C_R versus latitude. The corrections for HH and VV are plotted in Figure 10. The corrections for HH and VV are almost identical (within 0.01 dB). The difference between the highest and lowest value in the corrections in Figure 10 is approximately 0.7 dB. We expect this correction to be present in the X factor (see Figure 7), but this seems to be not fully the case. In Figure 7 we find a latitude dependence of X factor of approximately 0.35 dB, i.e., only half of the expected value. So, only half of the necessary orbit height correction appears in the X factor and an additional latitude-dependent correction is necessary to obtain a uniform response over the globe. We note that the precision of the orbit height knowledge has not been further verified at KNMI in other ways, but, as shown here, deviations of 10 or 20 km in height may cause noticeable backscatter effects that may vary along the orbit in a rather systematic manner.

Another identified cause may be in the settings of the Doppler signal windows, which are slightly offset due to a 20 degree rotation of the instrument look angle at any position. The associated Doppler variation due to the eccentric orbit needs further investigation in our view.

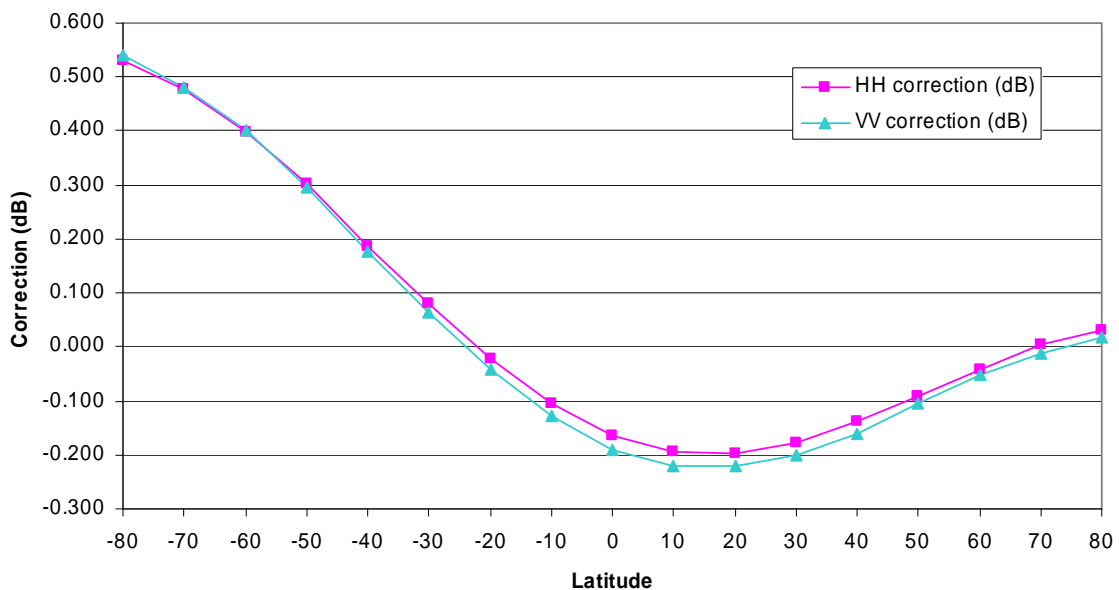


Figure 10: latitude dependent sigma0 corrections assuming an R^4 dependence.

Wind-SCATT, all Instruments, Globe, 20120101 to 20120229
 lsm@model=0, sst@model>=-1°C, quality_flags@knmi filtering
 Speed Bias, RMS Wind Vector Difference (Obs-Guess), function of latitude

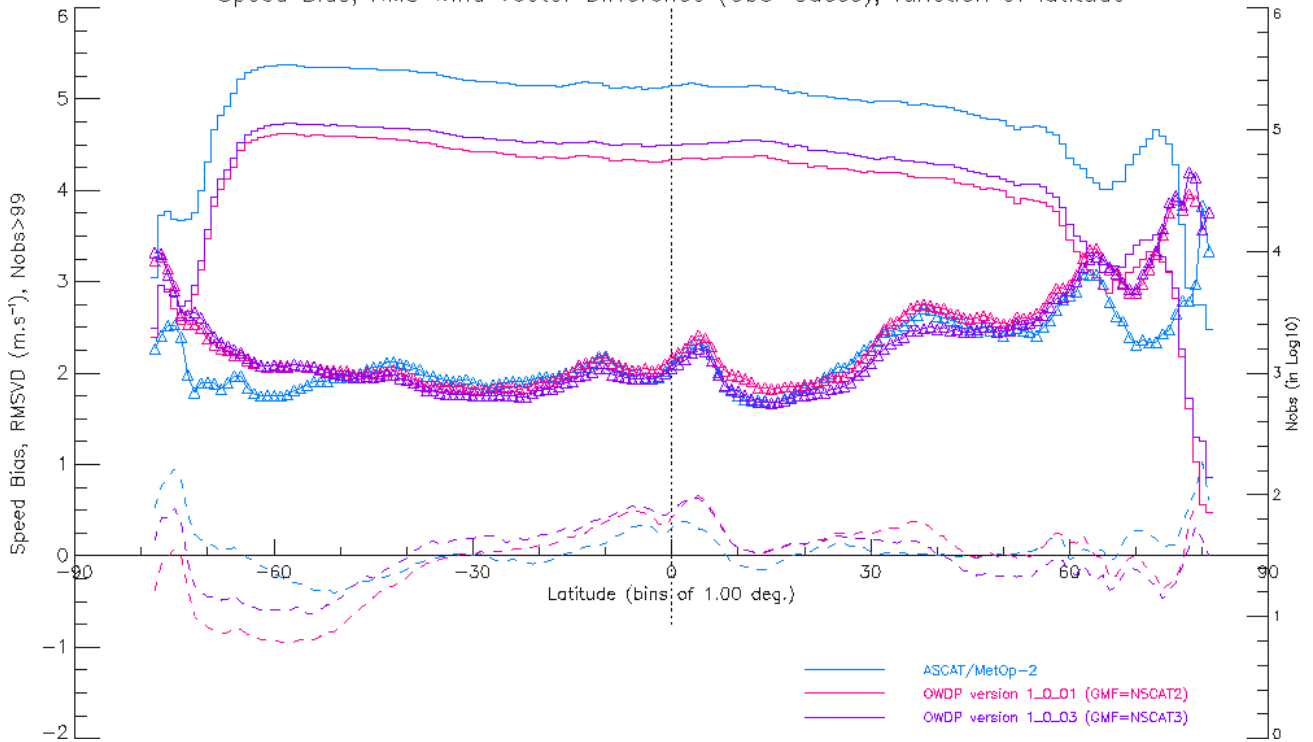


Figure 11: User verification of changes in OWDP as a function of latitude. OWDP version 1.0.01 has no latitude-dependent σ^0 correction and no high-wind correction by NSCAT3 (pink), while version 1.0.03 contains both these corrections (purple). The pink and purple dashed bias lines show mainly the effect of the latitude-dependent σ^0 correction. For reference ASCAT statistics are given too (blue). The plot collects statistics of wind differences between the Meteo France global NWP model and OWDP at each given latitude. The number of data on the right-hand-side (solid lines) varies due to QC, land and sea ice presence.

Several users verified the beneficial effect of the latitude-dependent backscatter correction in OWDP.

5. NWP Ocean calibration

NWP Ocean Calibration (NOC) is described in Stoffelen (1999) and Risheng et al. (2012), among others. Its main goal is to correct for stable linear gain biases in scatterometer systems. The schematic below describes the process which has been successfully applied for the ERS, ASCAT-A and ASCAT-B scatterometers. The procedure has initially not been applied at KNMI for Ku-Band pencil-beam scatterometers. A simplification with respect fan-beam scatterometers such as ERS or ASCAT may be in the fixed incidence angle of each beam and in its beam rotation, thus resulting in a uniform wind direction sampling. On the other hand, Ku-band scatterometers experience increased sensitivity to rain and increased sensitivity at low winds. The latter is problematic since at low wind speeds the GMF is more non-linear and the NWP input errors relatively larger (these are in absolute value rather independent of wind speed).

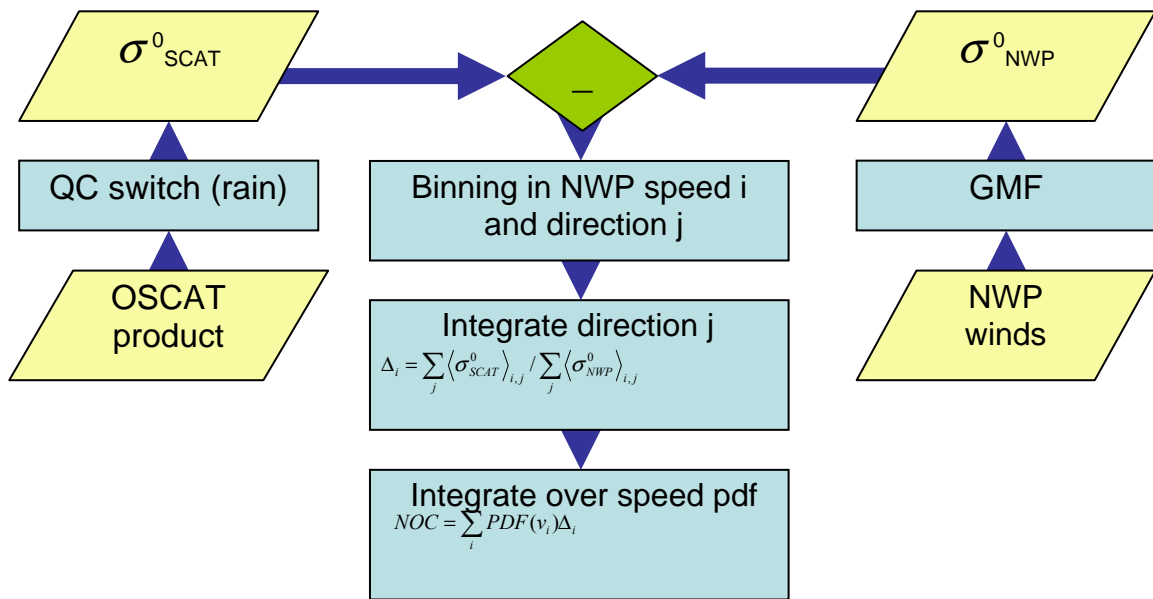


Figure 12: schematic of the NWP Ocean Calibration (NOC) procedure.

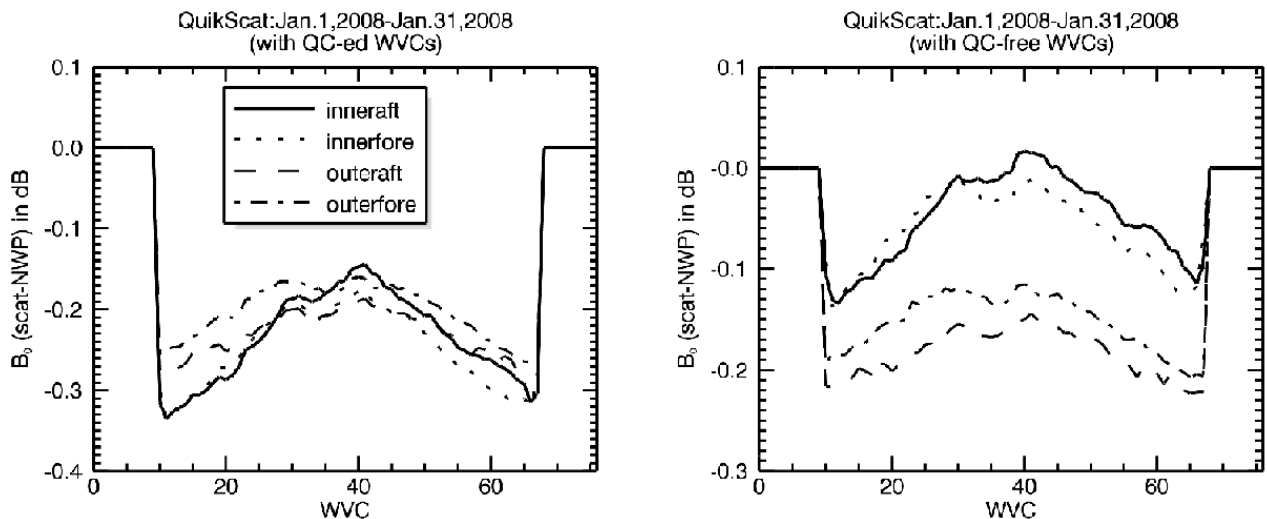


Figure 13: NOC of QuikScat backscatter data. Left panel with rain screening, right panel without.

Further intricate aspects of the NOC procedure reside in the binning of speed and direction, which bins need to be small enough to prevent discretisation errors, but large enough to allow adequate sampling in each bin. Moreover, when the mean backscatter at a given speed is computed, each wind direction bin should be weighted equally to limit errors due to integration

of the harmonic dependency. Due to the uncertainty in the input data, possible errors in the GMF and the non-linearity of the GMF, the NOC result may be biased. There are two ways to detect these biases. The first is through the GMF inversion in the scatterometer wind retrieval. The retrieved winds should show reduced biases and SDs against the reference NWP winds. The second way is through simulation of the NOC results. Detailed error analysis provides a reasonable model for the random uncertainties, e.g., using triple collocation (Vogelzang et al. 20) and backscatter noise modelling (Portabella et al, 2006). The simulation could use the NWP winds as truth and simulate corresponding true backscatter values. Then, noise may be added to both the true winds and backscatter, after which the projection of these uncertainties through the NOC procedure may be tested.

NOC was first applied to QuikScat data (Yun et al, 2012) as depicted above. In the left panel the KNMI QC has been used in the NOC results, whereas the right panel shows the rain contaminated results. The KNMI QC has a clear effect on the NOC results in making them consistent both among the fore and aft and inner and outer views, where in particular the inner beam (HH) backscatter is reduced, according to expectation. Nevertheless, a clear negative bias remains. However, this is in itself not surprising as the KNMI QuikScat winds were also biased low with respect to the ECMWF winds. Besides the bias, also a 0.1 dB WVC variation may be noted. It appears in both panels and therefore is unlikely due to rain effects and QC. Since the prime azimuth looking directions of all views vary rather systematically as a function of WVC, the variation may be due to NWP azimuth error. This is to be further investigated, but not of prime concern here.

The application of the inverse QuikScat NOC biases to the backscatter values before wind inversion has a rather neutral effect on the quality of the winds, although the former negative speed bias is removed.

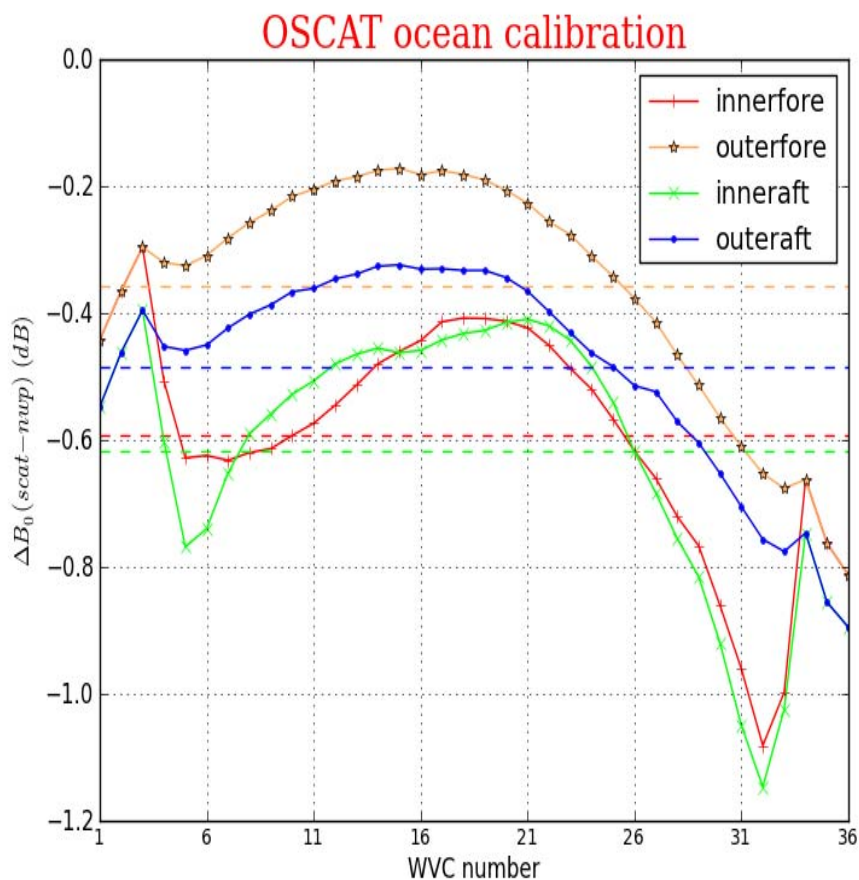


Figure 14: OSCAT NWP Ocean Calibration results. The dashed lines indicate the mean value for each view type.

Next, the NOC is applied to OSCAT data, but after applying the latitude-dependent correction as depicted above. Whereas the KNMI correction is -0.65 dB for both inner and outer, the NOC results indicate the outer beam correction should be about 0.2 dB higher. Results in the outer swath appear rather variable, since inner and outer views are mixed in the processing here, and these results are not further discussed. We note that the variation of the NOC results in the inner swath is much larger than for QuikScat, i.e., up to 0.7 dB for OSCAT and up to 0.2 dB for QuikScat. Moreover, the variation is rather asymmetric with respect to the middle of the swath for OSCAT, while QuikScat shows a symmetric pattern. It remains unclear how these differences are caused.

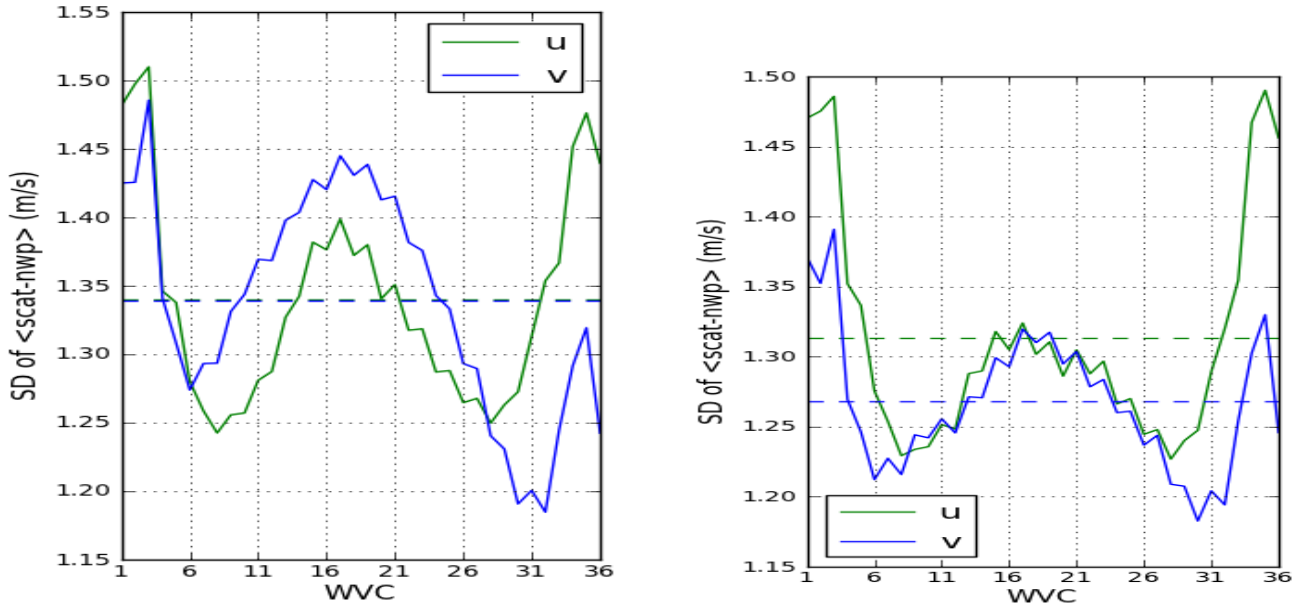


Figure 15: SD of OSCAT minus NWP wind component differences for operational products with 0.65 dB bias correction (left) and NOC bias correction (right).

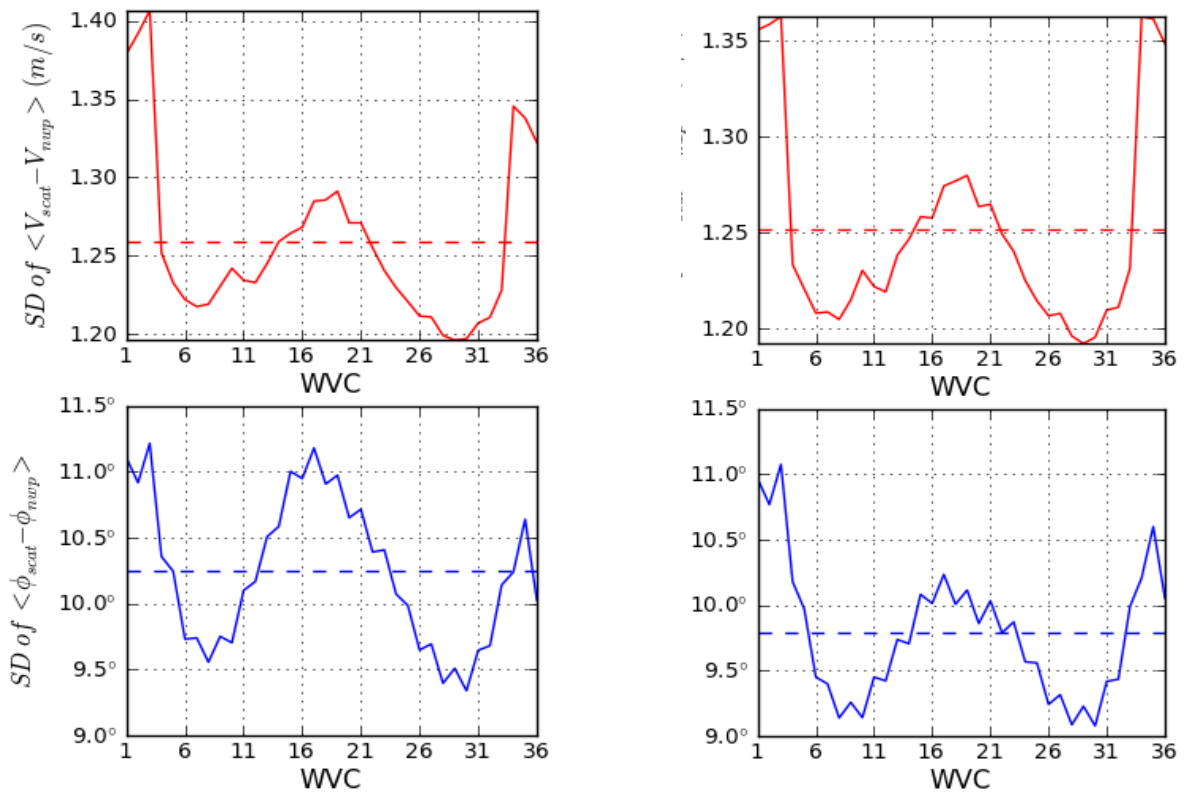


Figure 16: Left: SD of OSCAT minus NWP wind speed differences (top) and SD of OSCAT minus NWP wind direction differences (bottom) for operational products with 0.65 dB bias correction (left). Right: same as left, but with NOC bias correction.

Nevertheless, following the rather neutral experience with inverse NOC corrections in the QuikScat wind retrieval, one may expect beneficial effects after the correction of the much larger OSCAT NOC biases. Indeed, in the figure above a clear improvement is seen in both the west-to-east (u) and south-to-north (v) wind component differences between OSCAT and ECMWF NWP fields, particularly in the sweet and nadir swath parts. The figure below depicts the corresponding improvements in speed and direction differences between OSCAT and ECMWF. Most of the improvement in correspondence is achieved in the wind direction, whereas the wind speed differences are only modestly improved. The mean OSCAT minus ECMWF wind speed difference does not change much in magnitude and remains close to zero, though the bias pattern becomes more symmetrical after NOC (not shown).

6. NSCAT-3 GMF

IFREMER compared one month of Oceansat-2 wind data (November 2009) to in situ data from moored buoys. This study was done using the wind data computed by KNMI with OWDP. Various buoy data sets from Météo-France, UK MetOffice, NDBC, TAO, PIRATA and RAMA were used. Figure 17 shows an example of the results, both for Oceansat-2 and for ASCAT wind data. As expected, in version 1.2 wind speeds below 3 m/s do not occur. Moreover, the plots are in agreement with the results shown later on; a positive, increasing bias is seen at higher wind speeds. Therefore, the with respect to ASCAT systematically enhanced OWDP wind speeds above 15 m/s appear due to the NSCAT-2 GMF.

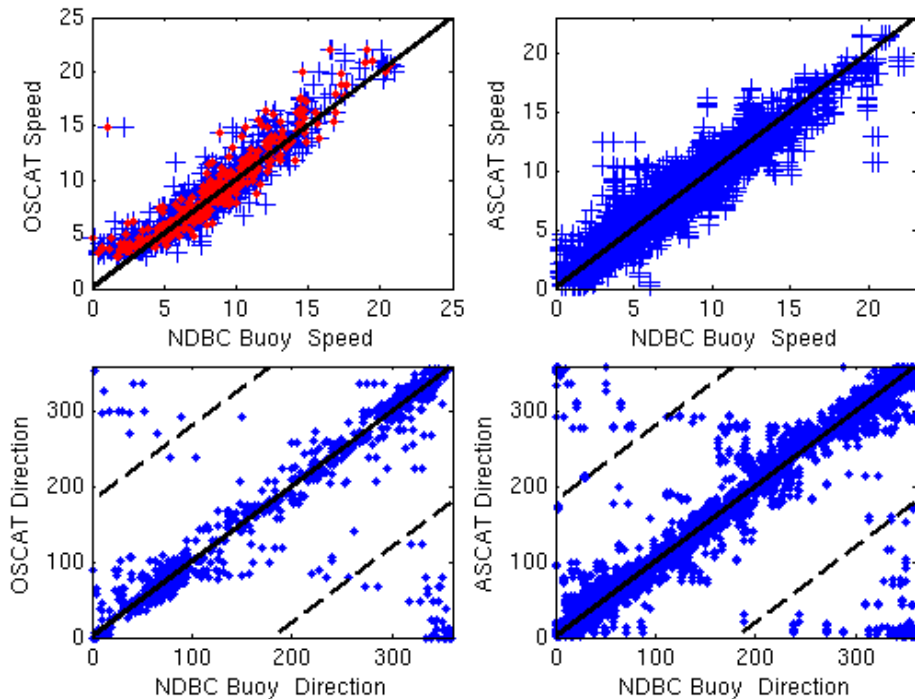


Figure 17: comparisons of buoy (NDBC) and scatterometer (OSCAT (1st column) and ASCAT (2nd Column)) wind speed (1st row) and wind direction (2nd row) for November 2009 by IFREMER.

The NSCAT-2 Geophysical Model Function was adapted for wind speeds above 15 m/s. The new GMF is called NSCAT-3. Below 15 m/s nothing was changed and the NSCAT-3 winds are identical to the NSCAT-2 retrieved winds. Above 15 m/s, a linear scaling of the wind speed was applied, starting with a zero correction at 15 m/s, a 2.5 m/s downward correction at 20 m/s, 5 m/s downward correction at 25 m/s and so on. This means that if a certain backscatter value results in a wind of 20.0 m/s in NSCAT-2, the same backscatter value will result in a wind of 17.5 m/s in NSCAT-3. The NSCAT-2 GMF lookup table was adapted in this way for all combinations of incidence and azimuth angles. This ensures that the fit in measurement (inversion) space of the backscatter quadruplets to the GMF will not change, only the retrieved speed changes. The high speed correction was tuned by comparing scatterometer wind speeds with ECMWF and buoy winds. We looked at the scatterometer wind speed bias versus the average scatterometer and background wind speed, background being ECMWF or buoy winds. Using the proposed GMF change, we obtain a rather flat bias, not only for OSCAT as will be shown in this report, but also for SeaWinds as we verified. Note that precise tuning of high speed winds is not easy. Due to the limited amount of available data above 15 m/s, the errors in the ECMWF and buoy winds are not very well known. Comparison to NOAA hurricane flight data is ongoing within the International Ocean Vector Winds Science Team (IOVWST).

7. Evaluation of winds

7.1. ECMWF model comparison

The contoured histograms in Figures 18 and 19 show statistics of the wind speed, wind direction (with respect to wind blowing from the North), and u (eastward) and v (northward) wind components. The scatterometer winds are compared with ECMWF forecast winds (3 to 18 hours ahead); the model winds are interpolated with respect to time and location. The ISRO L2B product wind speed (Figure 18, top left panel) is clearly biased low for wind speeds below approximately 5 m/s. The winds created with OWDP have less wind speed bias, but show a cut off below 3 m/s. This is due to the problematic (corrected) backscatter distribution, containing no σ^0 values below -40 dB.

The u and v wind component standard deviations for the ISRO L2B product are 1.87 and 1.76 m/s, respectively. For the OWDP product the u and v wind component standard deviations are 1.62 and 1.55 m/s, respectively, i.e., the OWDP product compares better to ECMWF winds than the ISRO L2B product. For the OSI SAF SeaWinds 25-km product, we found standard deviations of 1.28 and 1.40 m/s for a comparable data set, i.e., considerably lower values.

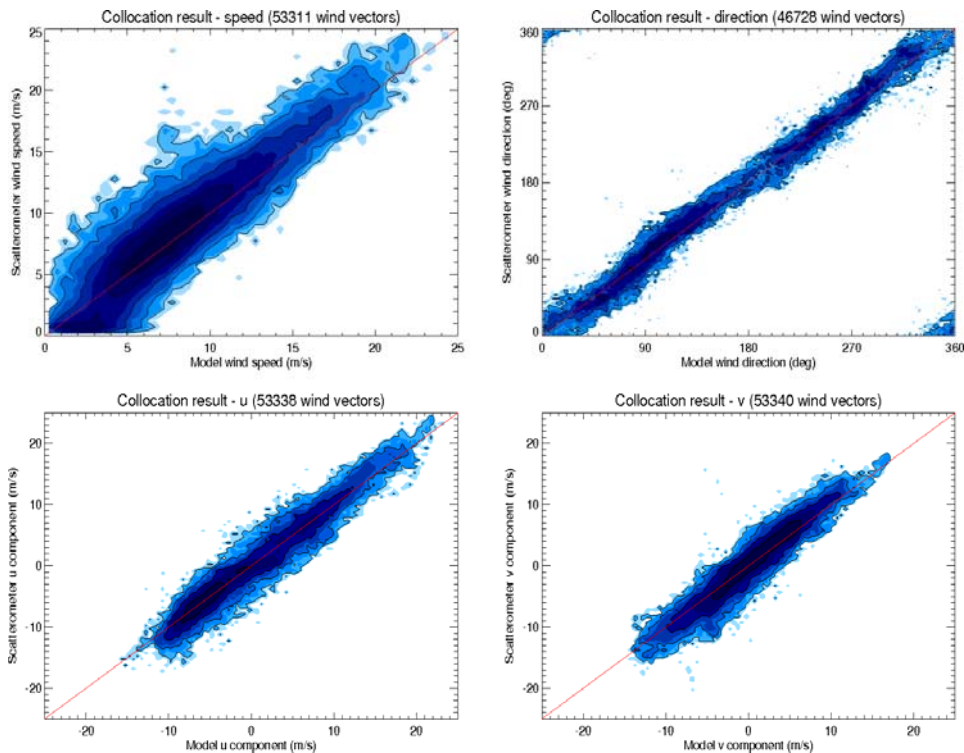


Figure 18: contoured histograms of Oceansat-2 winds from the ISRO level 2b product versus ECMWF forecast winds for 4 orbits (638-641) on 6 November 2009. Only wind directions for ECMWF and OSCAT speeds above 4 m/s are present in the joint wind direction distribution.

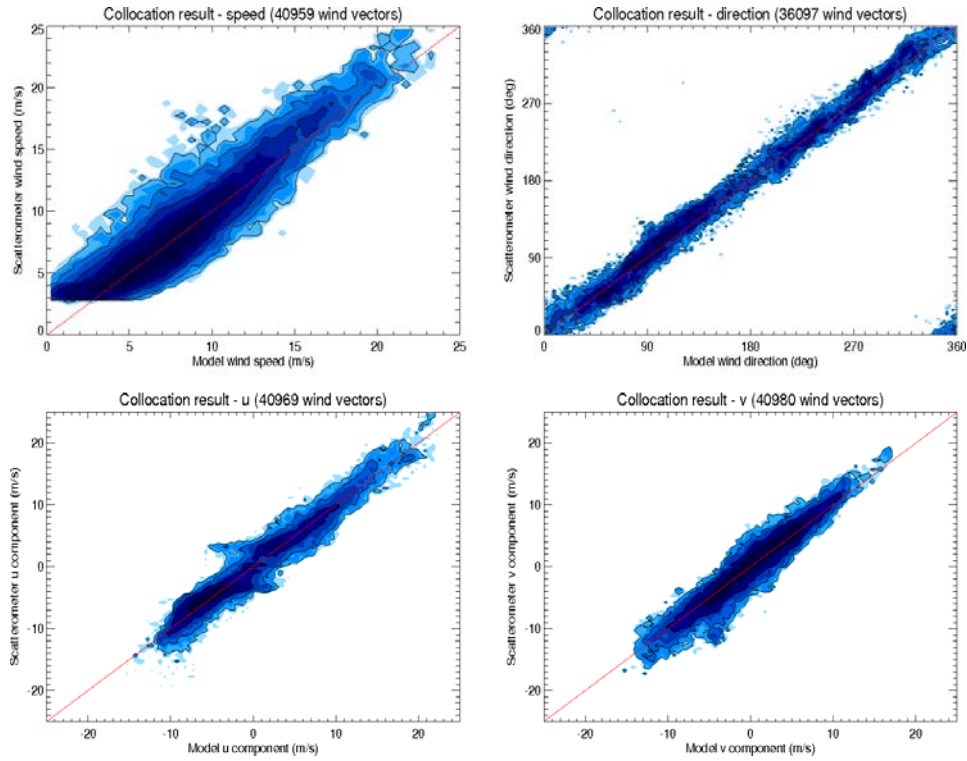


Figure 19: contoured histograms of Oceansat-2 winds from OWDP versus ECMWF forecast winds for 4 orbits (638-641) on 6 November 2009. A sigma0 correction has been applied (see text). Only wind directions for ECMWF and OSCAT speeds above 4 m/s are present in the joint wind direction distribution.

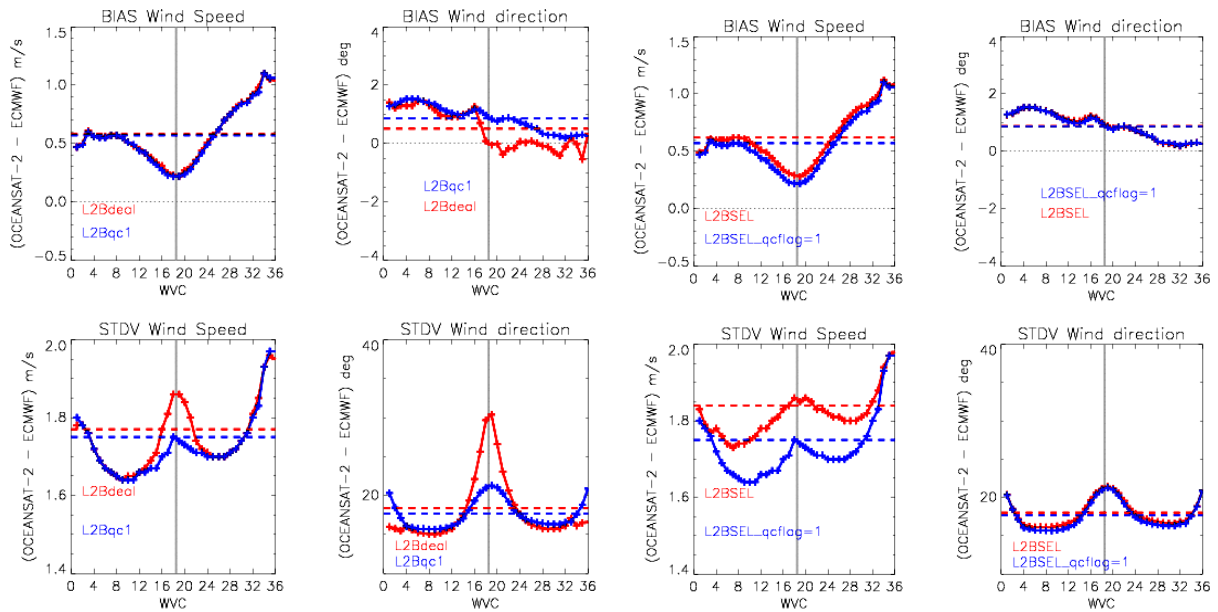


Figure 20: comparison of ISRO L2B winds with ECMWF model forecast winds. Left: ISRO-selected winds with no QC on flag (red) and insisting that Wind Quality Flag is equal to 1 (rain flagging attempted) (blue). Right: ISRO ambiguities closest to ECMWF wind (red) and ISRO-selected wind insisting that Wind Quality Flag is equal to 1 (rain flagging attempted) (blue).

ECMWF compared the version 1.2 ISRO L2B wind product to the forecast winds of the ECMWF model. Figure 20 shows WVC-dependent plots of wind speed and wind direction biases and standard deviations. The use of the Wind Quality Flag in the L2 product removes approximately 3% of the winds and results in slightly better statistics, mainly regarding to the wind speed standard deviation (left part of Figure 20). When the ISRO ambiguity closest to the ECMWF model wind is considered, the statistics are approximately as good as for the ISRO-selected winds (right part of Figure 20). A clear overall bias in wind speed together with a WVC-dependent slope occurs in all cases. This indicated systematically different backscatter values as a function of WVC, as was also noted in the discussion on NOC.

	ISRO L2B v1.3	OWDP v1.3	L2B v1.3 WVC 5-32	OWDP1.3 WVC 5-32	OWDP1.2 WVC 5-32	HY2A
Number	246699	268072	185364	219890	212427	715592
Bias (m/s)	-0.32	0.27	0.26	0.16	-0.37	0.01
SD speed (m/s)	1.45	1.29	1.27	1.35	1.34	1.45
SD dir. (deg.)	14.99	9.37	9.17	9.39	10.25	10.72
SD u (m/s)	1.75	1.31	1.78	1.30	1.32	1.46
SD v (m/s)	1.61	1.29	1.49	1.35	1.35	1.45

Table 1: Verification statistics against collocated ECMWF fields over a period of two days. Only wind directions for ECMWF and OSCAT speeds above 4 m/s are present in the wind direction differences.

The table above summarizes wind verification statistics as obtained against collocated ECMWF background winds over a given period of two days. The first row shows that OWDP generally delivers more winds than present in the ISRO L2B files. This is probably due to the use of the Brightness Temperature (BT) measurement of OSCAT that appears unstable. ISRO now developed a procedure for their QC, using calibrated BT. The three right-hand-side columns of the table show changes from ISRO version 1.2 to 1.3. Only WVCs 5-32 were processed initially at KNMI. Clearly, OWDP processes more reliable winds using version 1.3 inputs, which is due to the improved (corrected) backscatter distribution, particularly at low winds. The improved backscatter distribution furthermore results in clearly improved wind directions. Also the mean inversion residual (MLE) is reduced (not shown), which also suggests more consistent backscatter data in version 1.3.

The table also shows preliminary results for the Chinese HY2A scatterometer. The results were obtained with OWDP, but with HY2A L2A backscatter data corrected as follows:

- -1.7 dB σ^0 corrections for both inner and outer beams;
- -0.0001 linear outer beam correction.

Uncertainties remain in the interpretation of some of the flags and no detailed analysis has been performed on the processing characteristics, but these first preliminary results are very encouraging indeed.

7.2. Buoy comparison

The Oceansat-2 wind data have also been compared with in situ winds from moored buoys. The buoy winds are distributed through the Global Telecommunication System (GTS) and have been retrieved from the ECMWF MARS archive. The buoy data are quality controlled and (if necessary) blacklisted by ECMWF (Bidlot et al., 2002). We used a set containing approximately 150 moored buoys spread over the oceans (most of them in the tropical oceans and near Europe and North America) which are also used in the buoy validations that are routinely performed for the OSI SAF wind products (see the links on <http://www.knmi.nl/scatterometer/osisaf/>). A scatterometer wind and a buoy wind measurement are considered to be collocated if the distance between the WVC centre and the buoy location is less than the WVC spacing divided by $\sqrt{2}$ and if the acquisition time difference is less than 30 minutes. The buoy winds are measured hourly by averaging the wind speed and direction over 10 minutes. The real winds at a given anemometer height have been converted to 10 m equivalent neutral winds using the LKB model (Bidlot et al., 2002, Liu et al., 1979) in order to enable a good comparison with the 10-m scatterometer winds (Portabella and Stoffelen, 2009).

The buoy validation results in terms of standard deviations of wind speed, wind direction and u and v components are summarised in Table 2. From the first two data rows, it appears that more buoys are used in the OWDP collocations than in the ISRO L2B product collocations (158

versus 131 buoys). This is due to the fact that in the ISRO L2B product a quite conservative land mask is used and hence many buoys in coastal areas are ruled out. In the OWDP processor we apply land screening based on an ECMWF land-sea mask which is less strict, see section 2. Another difference between the ISRO L2B and OWDP products is that the outer swath is not processed in OWDP for version 1.2 ISRO inputs, resulting in a lower number of collocations.

In order to compare a shared set of winds from both products, the data sets have been collocated; see data rows 3 and 4 in the table below. When we mutually compare the first two rows and the row 3 with 4, respectively, it appears that the OWDP winds compare clearly better to the buoys in terms of speed and wind component standard deviations. The ISRO winds compare slightly better in terms of wind direction standard deviations. This is therefore due to the low winds, where the OWDP wind directions are degraded because of the deformed backscatter distribution with respect to QuikScat. The effects on wind speed and wind component quality remain limited due to the low speeds where the backscatter errors occur. Another feature arising is that both the ISRO winds and the OWDP winds improve when the data sets are collocated: compare row 3 with 1 and row 4 with 2, respectively. The collocated data set only contains winds that have passed both the ISRO and the OWDP quality control steps. Apparently both quality control algorithms have a good skill to reject low quality winds and in this respect they are complementary.

Since we know that there is an issue with the backscatter values below approximately -40 dB, we also computed the statistics for WVCs containing wind speeds of 6 m/s and higher, i.e. leaving out the data with low σ^0 values. The results are shown in data rows 5 and 6 of Table 2. It appears that the u and v statistics of the ISRO L2B product get worse (compare row 3 with 5), but the statistics of the OWDP winds slightly improve (compare row 4 with 6). Note that these OWDP winds achieve a vector-RMS difference with buoys below 3 m/s. Buoy vector errors on the 50-km scale are typically 2.0 m/s (Vogelzang et al., 2010), which leaves the OWDP vector error to about 2.0 m/s, well within the OSI SAF wind quality requirements.

	Speed (m/s)	Direction (degrees)	u (m/s)	v (m/s)
ISRO L2B, 131 buoys	1.46	23.56	2.38	2.35
OWDP, 158 buoys	1.37	23.91	2.27	2.20
ISRO L2B, 130 buoys, OWDP collocated	1.38	22.17	2.29	2.18
OWDP, 130 buoys, ISRO L2B collocated	1.25	22.82	2.11	2.06
ISRO L2B, OWDP collocated, ≥ 6 m/s	1.34	19.40	2.41	2.30
OWDP, ISRO L2B collocated, ≥ 6 m/s	1.33	16.67	2.02	2.12

Table 2: Oceansat-2 buoy validation results over November 2009 – May 2010 (version 1.2) in terms of standard deviation of OSCAT minus buoy wind differences. Only wind directions for buoy and OSCAT speeds above 4 m/s are present in the wind direction differences.

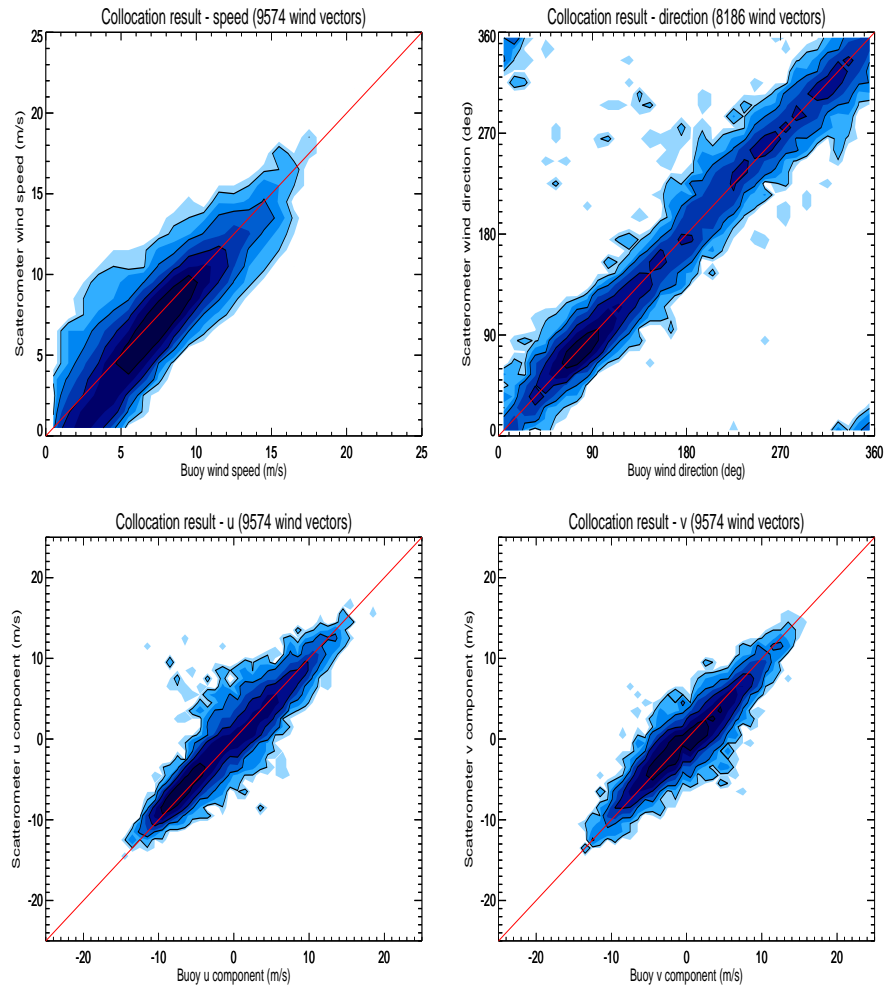


Figure 21: Joint distribution of 50-km ISRO L2B and buoy winds (version 1.3) from January to March 2012 for wind speed (upper left), wind direction (upper right), u component (lower left) and v component (lower right). Only wind directions for buoy and L2B speeds above 4 m/s are present in the joint wind direction distribution.

The figure above shows the joint distribution of collocated OSCAT and buoy winds over January to March 2012. The ISRO L2B winds in version 1.3 have improved with respect to version 1.2 (not shown). However, note that low speeds are biased low and that only a limited number of high speeds appear above 15 m/s and no wind speeds above 20 m/s. Moreover, the joint wind direction and wind component distributions show signs of ambiguity removal error.

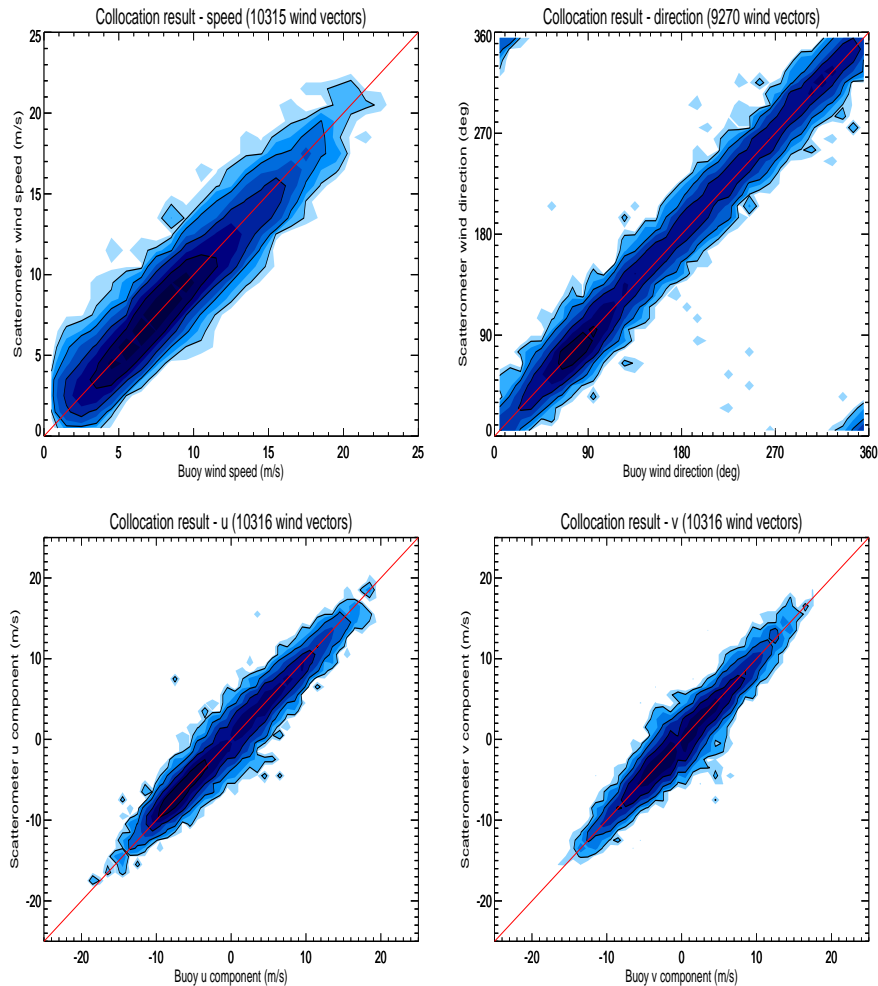


Figure 22: Joint distribution of 50-km OWDP and buoy winds from January to March 2012 for wind speed (upper left), wind direction (upper right), u component (lower left) and v component (lower right). Only wind directions for buoy and OWDP speeds above 4 m/s are present in the joint wind direction distribution.

Joint wind distributions were obtained for OWDP as well (see above) for the same period and buoys. Backscatter corrections include a constant correction of -0.65 dB and the latitude-dependent correction. We note that the introduction of the latter results in fewer rejections over the southern hemisphere (not shown). In version 1.3, we moved to a corrected GMF at winds above 15 m/s which reduce the OSCAT winds: NSCAT3. Nevertheless, OWDP does produce winds above 20 m/s and many winds in the 15-20 m/s range, unlike in the ISRO version 1.3 winds, where these winds are systematically rejected.

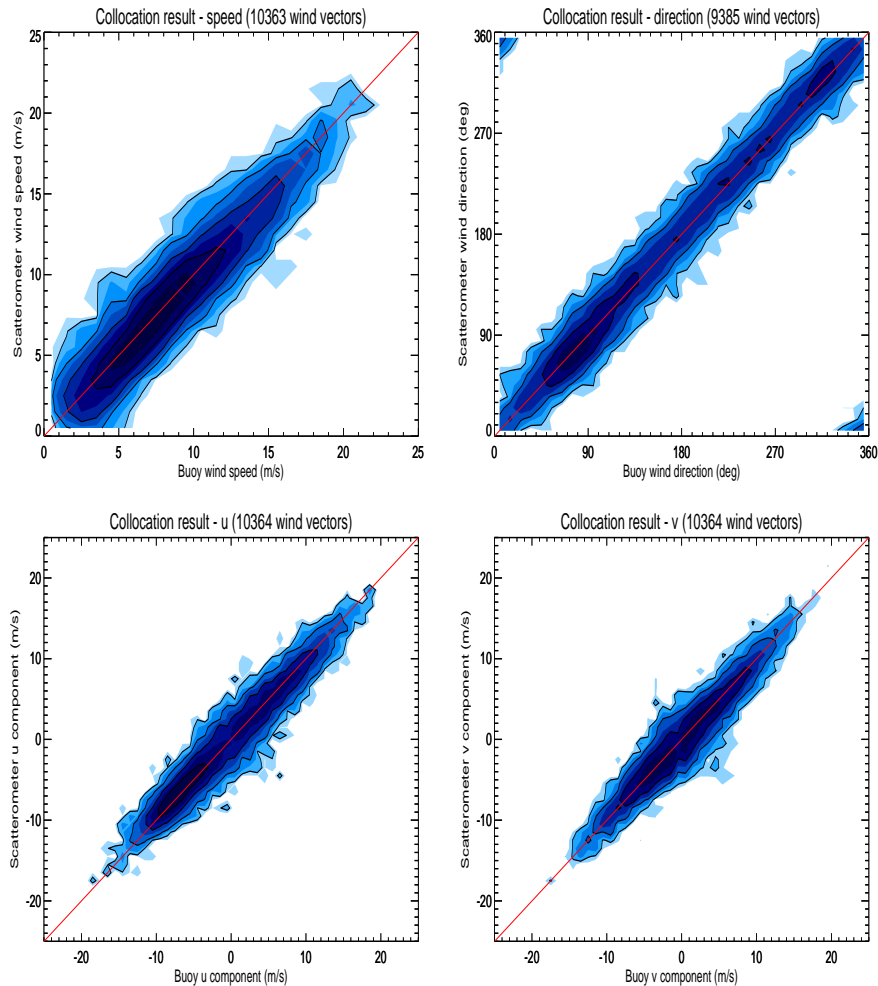


Figure 23: Joint distribution of 25-km OWDP and buoy winds from January to March 2012 for wind speed (upper left), wind direction (upper right), u component (lower left) and v component (lower right). Only wind directions for buoy and OWDP speeds above 4 m/s are present in the joint wind direction distribution.

Users request higher spatial resolution products. Given the good experience with the OWDP 50-km products, we started validation 25-km products. The L1B to L2A processing was done at KNMI using a processor developed by NOAA. The period and backscatter corrections are the same as before and also again the NSCAT-3 GMF is used. It appears that the OWDP QC scheme results in slightly less QC, but otherwise the distributions and statistical scores are very similar to the 50-km OWDP processing. This indicates, as expected, that the 25-km product does resolve some additional small-scale wind signal, but at the expense of introducing some noise.

	ISRO L2B v1.3	ISRO L2B @OWDP	OWDP1.3 @ISRO	OWDP* 50 km	OWDP* 25 km
Number	9574	7811	7811	10315	10363
Speed bias (m/s)	-0.43	-0.50	0.00	0.03	-0.11
SD speed (m/s)	1.36	1.28	1.11	1.18	1.18
SD dir. (deg.)	27.13	24.95	19.28	19.90	20.31
SD u (m/s)	2.46	2.27	1.64	1.91	1.87
SD v (m/s)	2.16	2.03	1.79	2.00	2.00

Table 3: Oceansat-2 buoy validation results over January to March 2012 (version 1.3) in terms of bias and standard deviation (SD) of OSCAT minus buoy wind differences. Only wind directions for buoy and OSCAT speeds above 4 m/s are present in the wind direction differences.

The above table summarizes the buoy wind comparisons of OSCAT processing version 1.3. The KNMI OWDP shows very good performance with limited QC, both at 50 km and at 25 km WVC processing. After collocation of the 50-km and 25-km OWDP products the statistics do not change to any significance. The version 1.3 ISRO L2B winds have a low bias at low speed, which integrates to a negative mean bias of about 0.5 m/s over all buoy collocations and an elevated speed SD with respect to the OWDP and buoy differences. The ambiguity removal errors, noted in the joint ISRO and buoy wind direction distribution above, do result in degradation of the wind direction SD scores. In discussing the joint wind distributions of OSCAT and buoys we noted the rejection of high winds in the version 1.3 ISRO winds. When the OWDP buoy collocations are collocated with the ISRO wind collocations (middle data column in the table), we note the improvement in the SDs of OWDP minus buoy differences, particularly for the u and v wind components. By inspection of the joint OWDP and buoy wind distributions above, we see no particular quality problem in these high winds, so rejection appears undesirable. So, rather than striving for the lowest overall differences between OWDP winds and buoys, we'd rather limit QC to physically unrepresentative cases of so-called confused sea state or rain.

ISRO uses the OSCAT BT for QC, which has not been calibrated. This is a known problem, which ISRO has mended. The improved ISRO QC, which will become available shortly, rejects about 5% of WVCs, similar to OWDP. It would be of interest to compare both QC schemes again following the above procedure of collocation.

7.3. Triple collocation

The triple collocation method (Stoffelen, 1998; Vogelzang et al., 2010) compares three sets of data with different characteristics. For scatterometer data, which may be viewed as a virtually instantaneous wind measure over an area of 50 km diameter, comparison is often made to moored buoy winds, but, although instantaneous values exist, in situ winds are essentially local and do not represent a 50-km size area as scatterometers may do. Comparison is also made to global NWP models, but these have generally rather poor spatial and temporal resolution as compared to scatterometers (Vogelzang et al., 2010) and thus cannot deterministically resolve the 50-km scale. Stoffelen (1998) introduced triple collocation and estimated spatial representation errors, further elaborated by Vogelzang et al. (2010). The latter estimates the wind errors on the scales resolved by the scatterometer, which we have repeated here for the 50-km OWDP winds.

	OSCAT SD(u) [ms ⁻¹]	OSCAT SD(v) [ms ⁻¹]	Buoy SD(u) [ms ⁻¹]	Buoy SD(v) [ms ⁻¹]	ECMWF SD(u) [ms ⁻¹]	ECMWF SD(v) [ms ⁻¹]
OWDP, all WVC	0.69	0.54	1.46	1.57	1.03	1.09
OWDP, WVC 5-32	0.67	0.51	1.46	1.57	0.99	1.10
OWDP, WVC 1-4,33-36	0.74	0.61	1.47	1.59	1.16	1.01
QuikScat 25-km	0.79	0.63	1.40	1.44	1.19	1.27

Table 4: OWDP OSCAT, buoy and ECMWF wind component error estimates by triple collocation over January to March 2012.

The table shows at first sight very similar results in all rows, i.e., the winds produced for QuikScat by the SeaWinds Data Processor compare well to the OSCAT winds by OWDP. This is very good news as it verifies the basic principle that was adopted in the European OSCAT Cal/Val AO project: if two scatterometers show the same (calibrated) backscatter distributions over the ocean, then, using an identical wind processor, the same quality wind distributions may be obtained. However, this only works with another premise, which is that the noise of both scatterometers is similar too. We noted some open problems on latitude dependence and WVC dependence of backscatter data, which do not appear dominant here. This could be due to the limited geographical and WVC sampling. One independent indication of the plausibility

of these scatterometer wind component errors is in the collocation of ASCAT and OSCAT winds within 25 km and one hour. Although this comparison is limited to around latitude 50S, the SD of OSCAT minus ASCAT wind speed differences is 0.9 m/s. If this difference was equally due to uncertainties in the OSCAT and ASCAT retrievals, then the OSCAT speed uncertainty would be 0.65 m/s, which is quite close to the value in the table. The obtained error estimates are clearly well within the EUMETSAT wind quality requirements.

Note that the QuikScat data is at 25-km sampling, whereas OSCAT WVCs are of 50 km size. This implies that the QuikScat winds should better resemble the local buoy winds than OSCAT does. Indeed buoy errors are smallest for QuikScat. To the contrary, 50-km OSCAT winds should better compare to ECMWF winds than 25-km SeaWinds does. Indeed, the results are consistent in this manner.

7.4. Future plans

The OWDP software is being released in the NWP SAF and operational NRT OWDP winds are processed and globally distributed in the OSI SAF at good quality.

Open issues remain in the NOC procedure which will be further tested and verified to arrive at a working procedure within 0.1 dB, if possible at all. After user request OWDP has been extended to process a 25-km product based on Level 1B data from ISRO and the NOAA L2A processing. This product will be compared with the ISRO 25-km winds and, as in the past, feedback will be provided to ISRO (and NOAA). Users are also interested in a coastal product and the limitations of processing near the coast should be investigated. Moreover, for ASCAT, KNMI has shown that structures at sea affect QC and wind climate. Similar effects are expected for Ku band systems, but this has not been tested in the scatterometer community. Bayesian sea ice screening is under development for OSCAT, but the Antarctic implementation awaits the definite correction of the latitude-dependent backscatter biases.

Within the European Union (EU) Global Monitoring for Environment and Security (GMES) programme marine core services are set up in a project called MyOcean (MyOcean, 2013). In the catalogue on the MyOcean web site global scatterometer winds from OWDP are being made available from KNMI. This concerns a so-called level 3 (L3) daily product, but which separates ascending and descending orbits to prevent time-of-day mixing in the product. It is planned to make available stress, curl and divergence products as well, besides a daily level 4 (L4) product that blends all available OSVW data with ECMWF winds and which is produced by IFREMER.

8. Applications

8.1. *Ocean Vector Wind Constellation*

The quality of the OSCAT winds is shown to be similar to the quality of the QuikScat winds processed at KNMI. The consistency between the OSCAT and SeaWinds data sets allows full user transparency in the use of any Ku-band pencil-beam scatterometer and the construction of consistent long-term climate-quality wind data sets.

Another important asset of the OceanSat-2 vector winds is its local ascending equator crossing time (LTAN) of 00:00, which essentially determines the time of day of local satellite overpass, i.e., around 00:00 LST and 12:00 LST (descending). The wind at sea is extremely variable due to processes such as mesoscale convective systems, frontogenesis, ocean eddy-scale air-sea interaction and the diurnal cycle, the latter of which is most prominent in the coastal zones. The time scales of these processes vary from less than hours in case of convection, to daily and weekly for ocean eddy-scale processes. The World Meteorological Organisation (WMO) maintains a data base of user requirements for diverse applications in meteorology and oceanography (it coordinates with the IOC). It may not be surprising that many applications require 3- or 6-hourly coverage of Ocean Surface Vector Winds (OSVW). One satellite is not able to fully capture these processes and requirements.

The Committee on Earth Observation Satellites (CEOS) OSVW Virtual Constellation (VC) answers the call for frequent, standardized, NRT satellite winds. The following constellation capability is noted in terms of general temporal coverage:

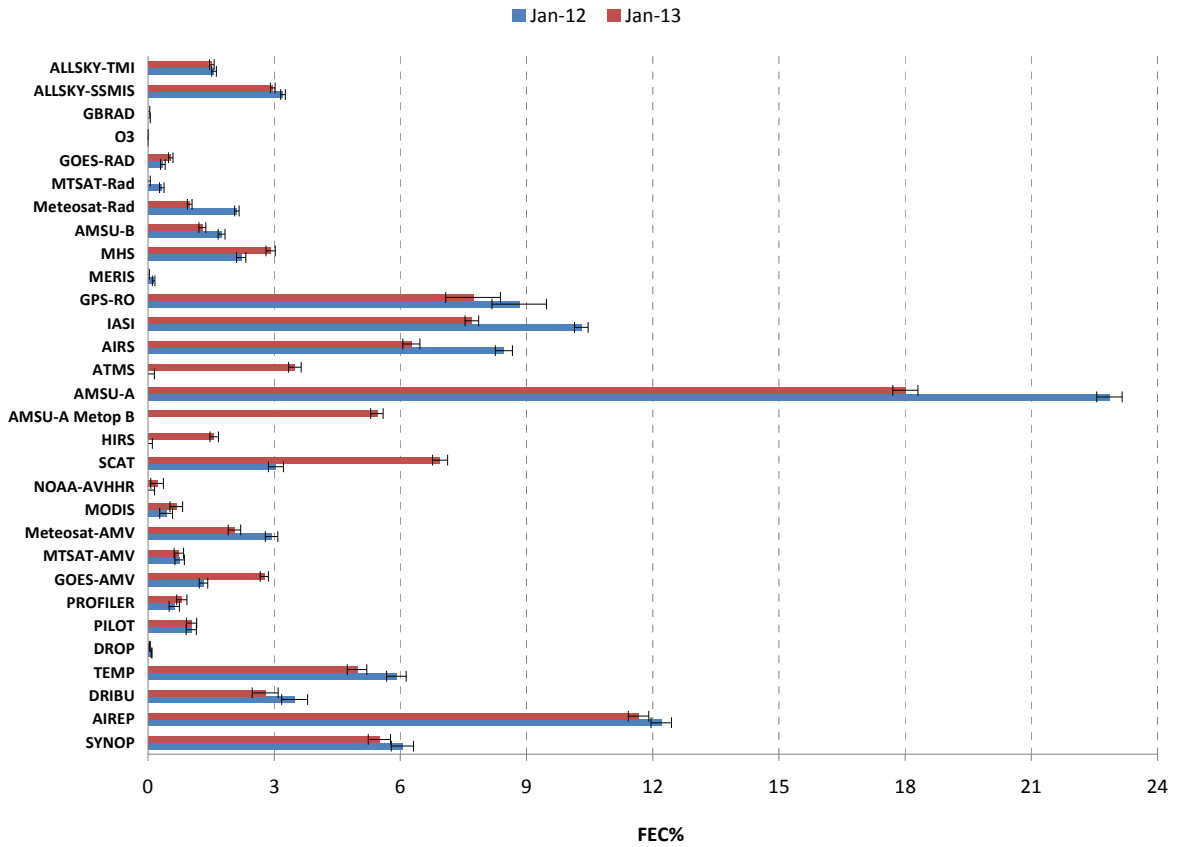
- 0:00 LST & 12:00 LST: OSCAT;
- 6:00 LST & 18:00 LST: from the Chinese HY-2A scatterometer HSCAT or for wind speeds > 8 m/s from WindSat by the USA Naval Research Laboratory (NRL);
- 9:30 LST & 21:30 LST: Advanced Scatterometers ASCAT-A and ASCAT-B carried by the Metop-A and MetOp-B meteorological satellites, operated by the European Organisation for the Exploitation of Meteorological Satellites (EUMETSAT);

In each of the three LTAN configurations follow-on instruments are planned (CEOS OSVW VC, 2013). Therefore, applications may be developed that exploit such configuration with a midnight, early morning and mid-morning satellite. Note that for some of the applications that provide maritime warnings for safety of property and mankind, timeliness of satellite data is of prime importance, but not always provided yet.

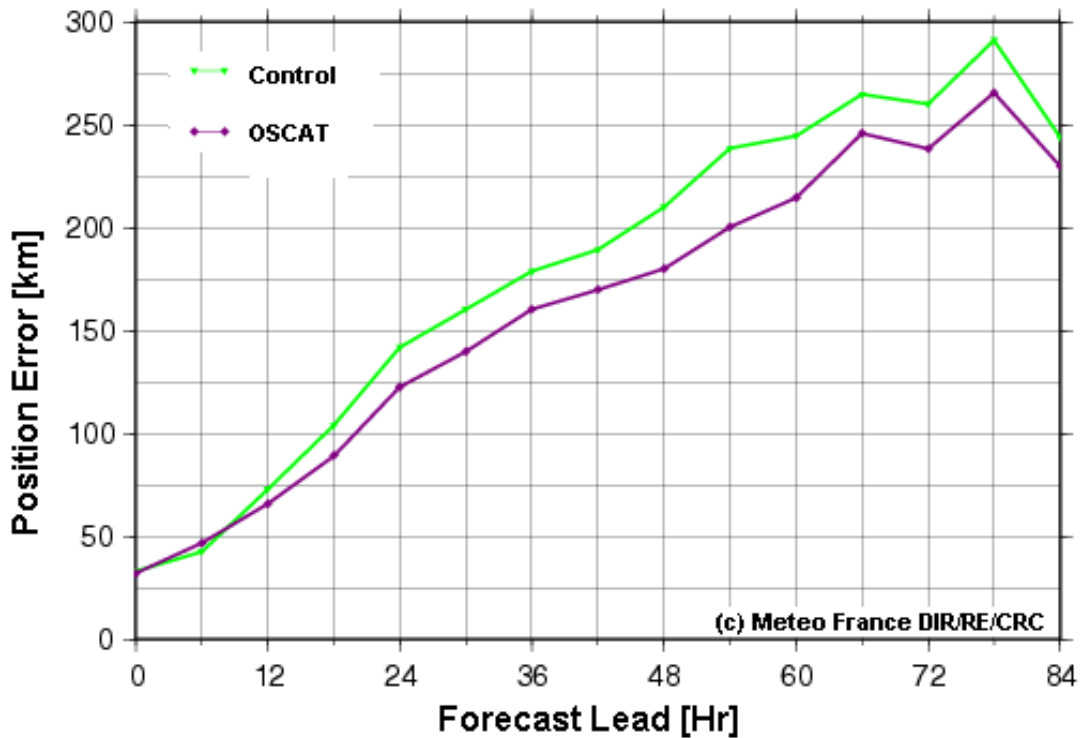
8.2. *Numerical Weather Prediction*

Over the past decades larger computers have brought improved atmospheric circulation model sampling the atmosphere at unprecedented detail. These models are successfully used in Numerical Weather Prediction (NWP), but do require a significant amount of tuning to capture the mean effect of unresolved processes, such as mixing processes, clouds, rain or gravity waves. By systematically comparing NWP outputs to spatially or temporally coherent observations, much can be learned about the representation and qualities of NWP models and observations. Both have led to a better use of in particular satellite observations in this century. Since its inception in 1978, the European Centre for Medium-range Weather Forecasts (ECMWF) has been able to extend the range of a given forecast quality by one day in each decade. Today, its quality is largely determined by satellite (sounder) data and by consequence forecast skill in the southern hemisphere equals forecast in the northern hemisphere.

The EUMETSAT NWP SAF hosts the most complete scatterometer winds monitoring site and hosts information on scatterometer data assimilation procedures (NWP SAF, 2013). The aim of the monitoring site is to highlight differences between observed scatterometer winds and NWP model estimates of the equivalent-neutral 10-m winds. A key component is the provision of a 3-year rolling archive of monthly monitoring plots, which allows the inspection of differences between different model versions and different observation processing versions (e.g., the



a)



b)

Figure 24: OSCAT NWP impact:

- a) Impact at ECMWF of assimilated observations on Forecast Error Reduction (FEC) with (Jan 2013) and without (Jan 2012) OSCAT scatterometer winds assimilated; "SCAT" includes only ASCAT-A in both years, since ASCAT-B was not operational yet; OSCAT and ASCAT are complementary (Cardinali, 2009);
- b) Mean position errors (of MSLP minimum) of the 2011/2012 Tropical Cyclones in the south-west Indian Ocean as forecast with the regional Aladin Réunion NWP model. An experiment with OSCAT winds (purple) is compared to a control experiment without OSCAT winds (green). (Dominique Mékiès, , 2013)

introduction of the latitude-dependent backscatter correction. It is hoped that the monitoring site will become a useful resource for the data producers and users alike. The site's NWP section moreover hosts information on how scatterometers are assimilated at the UK MetOffice, Environment Canada, the Japanese Meteorological Agency and ECMWF. Other NWP centres are welcome to provide their procedure too for hosting it on the NWP SAF site.

ECMWF started the ingestion of OSI SAF OceanSat-2 L2B winds in their Integrated Forecasting System (IFS) in June 2012 to allow passive monitoring of the data. They noted that the latitude-dependent bias correction introduced in the OWDP successfully removed a speed bias that has been detected in the SH earlier on. To avoid any mean differences between the ECMWF model and scatterometer winds, ECMWF applies a global wind speed bias correction before wind assimilation. Winds are assimilated up to 25 m/s.

Today, the first Indian instrument data assimilated at ECMWF is from OSCAT, since commencement of its operational assimilation in December 2012. Globally, a neutral impact on the usual forecast scores is achieved, but it results in a more redundant and stable system. In a NWP wind impact study the impact of scatterometer winds have been investigated during the 2010 Tropical Cyclone (TC) season. It is found that scatterometer winds have a beneficial impact on the analysis and forecasts in tropical storm areas. Forecast improvements in TC track were noted. The Laboratory of the Atmosphere and Cyclones (LACy), mixed unit CNRS - Météo France at La Réunion Island in the south-west Indian Ocean, achieved impressive beneficial impacts on tropical cyclone forecasts with OSCAT. Using a dedicated regional NWP model, Aladin-Réunion, they ran a control experiment over the 2011/2012 cyclone season and compared it to an experiment where OSI SAF OSCAT winds were assimilated. The figure below shows that the position errors of the Mean Sea-Level Pressure (MSLP) minima are much reduced, extending the forecast quality at 30-hour range by between 6 and 12 hours.

Meteo France assimilates the NRT OWDP winds since autumn 2012. Also, the UK MetOffice reports beneficial impact of OSCAT winds on their global NWP model and provides a detailed account of the complementarity of OSCAT winds with ASCAT and WindSat winds in their NWP data assimilation and forecasting system (Cotton, 2013). OSCAT winds are operationally used at the UK MetOffice since January 2013.

The figure above shows the monitoring by the MetOffice of the OWDP winds version before and after the latitude-dependent backscatter bias correction and introduction of NSCAT3. The speed bias in the upper plot occurred over the same region in all seasons. OceanSat-2 OWDP winds also being used for NWP by e.g., KNMI, DWD, Met.No, Met. Portugal, Spain, Italy, Japanese Meteorological Agency, Bureau of Meteorology (Australia), Env. Canada, the USA Naval Research Laboratory, ENPE in Brazil, South Africa, HMC Russia, etc.. However, whether these services are operational in these places is generally unknown.

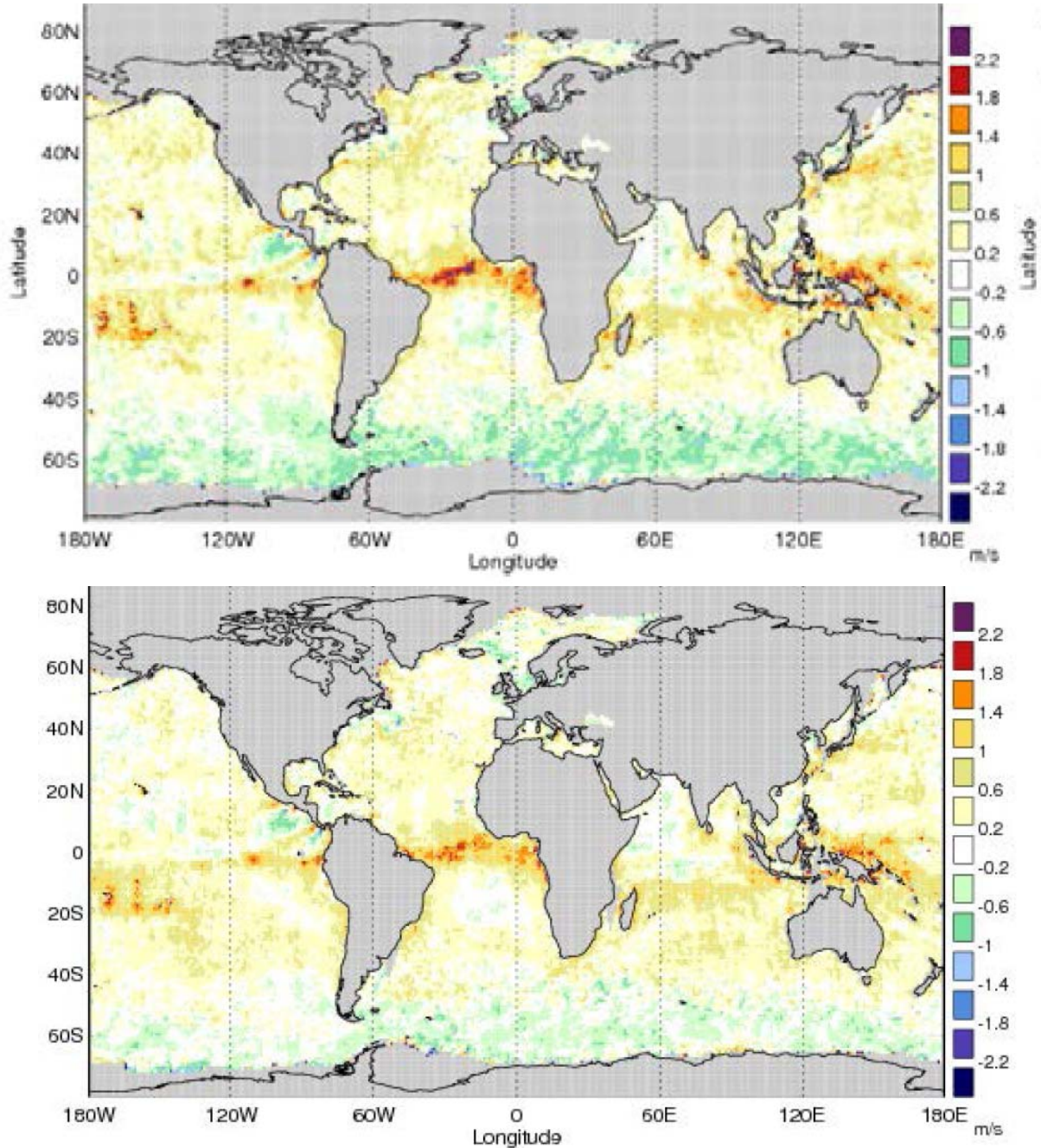


Figure 25: OWDP speed bias against the global UK MetOffice NWP model (background) in March 2012 for the OWDP version without latitude-dependent backscatter bias correction and NSCAT2 GMF (top) and for the OWDP version with latitude-dependent backscatter bias correction and NSCAT3 GMF.

8.3. Other Applications

The EU MyWave project runs parallel to the EU MyOcean project and too provides marine core services, but only for ocean waves. Thus, MyWave is a pan-European concerted and integrated approach to operational wave modelling and forecasting and complements the GMES MyOcean services. The main goal of MyWave is to lay the foundation for a future Marine Core Service that includes ocean waves, so it undertakes to (i) increase the use of earth observations by improving data processing algorithms and data assimilation systems, (ii) improve the physics in current wave models and provide a framework for coupled model systems (atmosphere/waves/ocean), (iii) establish a new standard for probabilistic wave forecasts based on ensemble methods and (iv) derive standard protocols for validation of products.

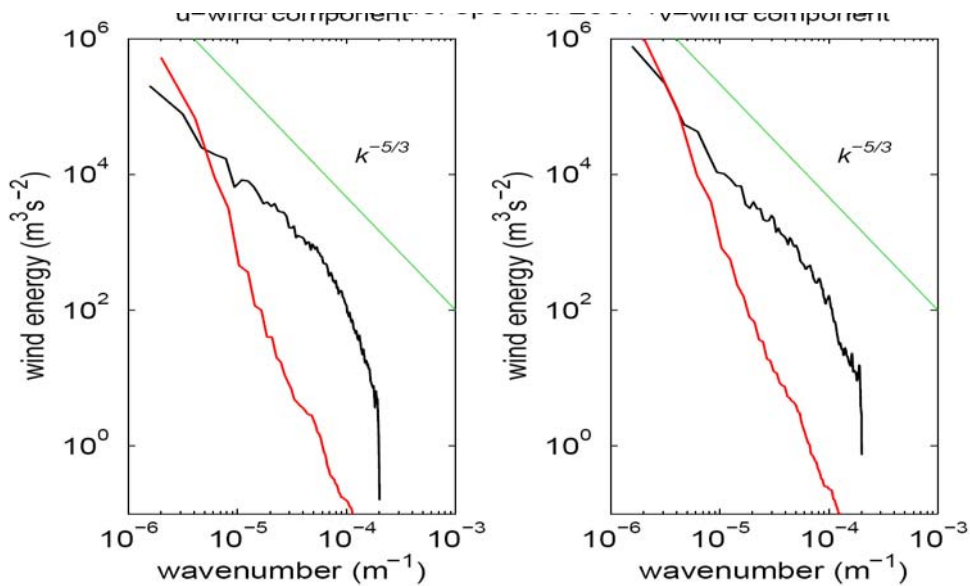


Figure 26: u (left) and v (right) wind component spatial wave-number spectra of collocated ECMWF (red) and HARMONIE (black) wind fields. The theoretical wind spectrum slope as anticipated by Kolmogorov is given in green.

The Dutch contribution to MyWave includes application of a non-hydrostatic km-scale model, HARMONIE, over a local target area including the North Sea. OSCAT and ASCAT scatterometer winds will be assimilated into HARMONIE and its effect on the wave model SWAN, coupled hourly, will be investigated with the Dutch DeltaRes institute. In the figure above, a wave number of 10^{-4} m^{-1} corresponds to a spatial scale of 10 km. So, the wind energy variance on scales between 10 and 100 km is very different in the global ECMWF and regional HARMONIE models, with grid sizes of 16 km and 2.5 km respectively. It will be investigated what the effect of mesoscale forcing is on the wave model outputs, with and without satellite data assimilation.

Besides waves, surges are another concern for delta areas like the Netherlands. For population safety national forecasting agencies have invested interests in more reliable storm surge forecasting models. KNMI participates in an European Space Agency (ESA) project called eSurge. Its objective is to bring together the wind surge community for capacity building and promote the use of earth observation (EO) data herein. It involves training about how best to exploit EO data and shows how forecasting models can be improved after the assimilation of EO data.

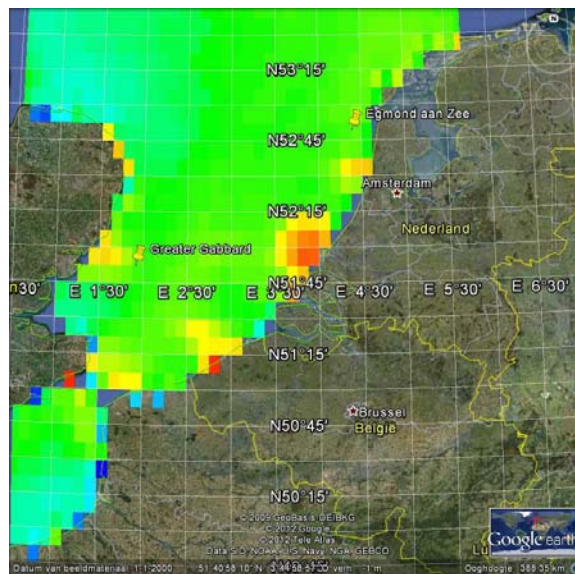


Figure 27: ASCAT scatterometer wind speed climatology in the southern part of the North Sea. The scale runs from 7 (blue) to 12 (red) m/s.

The objective of the EU NORSEWInD project was to obtain a wind climatology for the benefit of planning off-shore wind farms. The figure above shows an example climatology for the southern part of the North Sea with apparent high variability near the coast. However, grid boxes right near the coast are hampered by poor sampling. More worrying is the bright spot near 4E and 51N at the entry of the Rotterdam harbour, where scatterometer winds are much elevated at good sampling. This is due to corner reflections on the (over a hundred) container ships that are anchored up to 60 km away from the coast line. At low winds the scatterometer signals are most disturbed and the QC in the wind processing discards mainly low winds. Nevertheless, it needs to be checked (i) whether undetected corner reflections enhance the winds, (ii) how to improve detection and (iii) how to deal with scatterometer QC in climate records. Corner reflections in scatterometer data have not been studied for Ku-band systems, but seem equally probable theoretically. In a follow-on of the EU NORSEWInD OSCAT winds may play a role and corner reflections will be a topic. A project called Off-shore Wind India (OWI) is being defined with Indian and European partners.

8.4. Training

New EO techniques lead to applications once operational routines are adapted from within. Training of marine meteorologists, oceanographers, climate researchers and NWP users will be essential to achieve this. At KNMI some on-line resources have been collected:

- Training Course Applications of Satellite Wind and Wave Products for Marine Forecasting, <http://vimeo.com/album/1783188> (video)
- Forecasters forum, <http://training.eumetsat.int/mod/forum/view.php?f=264>
- Xynthia storm case, <http://www.eumetrain.org/data/2/xynthia/index.htm>
- EUMETrain ocean and sea week, http://eumetrain.org/events/oceansea_week_2011.html (video)
- NWP SAF scatterometer training workshop, http://research.metoffice.gov.uk/research/interproj/nwpsaf/scatterometer/data_assimilation_workshop/
- Use of Satellite Wind & Wave Products for Marine Forecasting, <http://classroom.oceanteacher.org/course/view.php?id=103>
- Satellite and ECMWF data visualisation, http://eumetrain.org/eport/smhi_12.php?

9. Conclusions

Wind data from India's OceanSat-2 scatterometer have proven to be a valuable resource in the international constellation of operational meteorological satellites. In particular, its local equator crossing time makes its data very complementary to other surface wind satellite data, allowing to depict processes such as the diurnal cycle or atmospheric mesoscale convection. In this light, the NRT capability implemented by ISRO led to the first Indian satellite instrument data be operationally assimilated in several European NWP models, including ECMWF's. Following these achievements, we look forward to the continuation and follow-on of this successful mission.

OceanSat-2 scatterometer (OSCAT) backscatter and wind data have been evaluated in response to the ISRO Announcement of Opportunity OceanSat-2 Cal/Val call. The backscatter data were found to be of a stable quality and an excellent starting point for the analyses described in this report. Based on the SeaWinds Data Processor (SDP), the Oceansat-2 Wind Data Processor (OWDP) has been developed to produce winds. OWDP adopts some backscatter corrections in which case it indeed achieves consistency between the OSCAT and SeaWinds data sets. This result is very important, as the methodology adopted here then allows full user transparency in the use of any Ku-band pencil-beam scatterometer and the construction of consistent long-term climate-quality wind data sets. The quality of the OSCAT winds is indeed shown to be similar to the quality of the QuikScat winds processed at KNMI with close verification to buoys and NWP models.

The ISRO and OWDP winds have been compared to ECMWF model and buoy winds. The ISRO wind data quality is reasonable. Ad hoc calibration to achieve SeaWinds backscatter levels allows wind processing by well-tuned SeaWinds wind processing modules and results in good quality winds for OWDP, both at 50-km and 25-km size WVCs. The NRT OWDP winds of the OSI SAF passed the EUMETSAT Operational Readiness Review and the OWDP package review for its full release by the NWP SAF is completed.

The collaboration with and at ISRO has been very effective. This applies to the setup of a NRT data stream to Europe and the USA, to the interactions with an international cal/val team from these countries (Jelenak et al., 2012; Jaruwatanadilok et al., 2012), but most in particular to the prompt internal response and resolution of remaining issues among the different contributing groups at ISRO. This resulted in an OSCAT processing version 1.3 at ISRO, which showed correction of the backscatter processing at low backscatter values in particular, which has further improved the low winds processing. Moreover, work is ongoing to further improve the OSCAT processing, a.o., related to the BT calibration and to the remaining latitude- and WVC-dependent biases. We look forward to further analyze the improvements in the data products.

It has become clear that India's OceanSat-2 scatterometer wind data are a valuable resource in the international constellation of operational meteorological satellites. In particular, its local equator crossing time makes its data very complementary to other surface wind satellite data, allowing to depict processes such as the diurnal cycle or ocean mesoscale convection.

Given the large number of operational users, quality assurance issues are at stake. Changes in the instrument, satellite or ground segment performance should be closely monitored and prompt or, if known a priori, advance notifications should be send to the users. Both monitoring and notification services are in place in Europe and we trust that these may be further connected to similar ISRO services.

Acknowledgements

The Oceansat-2 scatterometer L2A and L2B data were kindly provided by ISRO. We are particularly grateful for their development of a NRT capability benefitting many of the applications described in this report. The prototype OSCAT Wind Data Processor (OWDP) was developed in the EUMETSAT NWP SAF and the validation work was done in the OSI SAF. We are grateful to Jean Bidlot of ECMWF for helping us with the buoy data retrieval and quality control. Last but not least, we much enjoyed working on OSCAT in an international cal/val team comprising scientists from several ISRO divisions, from NASA, NOAA, and EUMETSAT; thanks to all. Special thanks to NOAA for providing their L2A processor. Yun Risheng worked as visiting scientist at KNMI supported by the Chinese Academy of Sciences on NOC. The enthusiasm of the home institutes supporting us scientists in this work is also much appreciated.

References

- Bidlot J., D. Holmes, P. Wittmann, R. Lalbeharry, and H. Chen (2002), Intercomparison of the performance of operational ocean wave forecasting systems with buoy data, *Wea. Forecasting*, vol. **17**, 287-310
- CEOS OSVW VC, 2013, http://www.ceos.org/index.php?option=com_content&view=category&layout=blog&id=73&Itemid=72
- Cotton, James, 2013, FRTR572 "Assimilating scatterometer winds from Oceansat-2: impact on Met Office analyses and forecasts", <http://www.metoffice.gov.uk/media/pdf/7/j/FRTR572.pdf>
- De Chiara, Giovanna, Peter Janssen, IOVWST 2012, Utrecht, the Netherlands, 12-14 June 2012, Assimilation of Scatterometer Winds at ECMWF, http://coaps.fsu.edu/scatterometry/meeting/docs/2012_meeting/Meteorology/IOVWST2012_DeChiara.pdf
- eSurge, 2013, <http://www.storm-surge.info/esurge>
- Jaruwatanadilok, Sermsak, Bryan W. Stiles, Alexander Fore, R. Scott Dunbar and Svetla Hristova-Veleva, OSCAT backscatter stability evaluation using ocean and natural land targets, IOVWST 2012, Utrecht, the Netherlands, 12-14 June 2012, http://coaps.fsu.edu/scatterometry/meeting/docs/2012_meeting/First%20results/OSCAT%20backscatter%20drift%20evaluation%20using%20ocean%20and%20natural.pdf
- Jelenak, Zorana, Seubson (Golf) Soisuvann and Paul Chang, OSCAT @NOAA: Update, IOVWST 2012, Utrecht, the Netherlands, 12-14 June 2012, http://coaps.fsu.edu/scatterometry/meeting/docs/2012_meeting/First%20results/ZJelenak_OSCAT_NOAA_IOVWST_final.pdf
- Leidner, S.M., Hoffman, R.N. and Augenbaum, J. (2000), SeaWinds Scatterometer Real-Time BUFR Geophysical Data Product User's Guide, Version 2.3.0.
- Liu, W.T., K.B. Katsaros, and J.A. Businger (1979), Bulk parameterization of air-sea exchanges of heat and water vapor including the molecular constraints in the interface, *J. Atmos. Sci.*, vol. **36**, 1979.
- Mékiès, Dominique, 2013, Météo-France La Réunion, LACy, personal communication.
- MyOcean, 2013, www.myocean.eu
- NORSEWInD, 2013, www.norsewind.eu
- NWP SAF, 2013, http://research.metoffice.gov.uk/research/interproj/nwpsaf/scatter_report/index.html, http://research.metoffice.gov.uk/research/interproj/nwpsaf/scatter_report/monthly_mon.html,
- Padia, K. (2010), Oceansat-2 Scatterometer algorithms for sigma-0, processing and products format, Version 1.1, April 2010.
- Payan, Christophe, and Hervé Benichou, Scatterometer winds at Météo-France, , IOVWST 2012, Utrecht, the Netherlands, 12-14 June 2012, http://coaps.fsu.edu/scatterometry/meeting/docs/2012_meeting/Meteorology/payan_scattwindsuse_meteorology.pdf
- Portabella, M. and A.C.M. Stoffelen (2009), *On Scatterometer Ocean Stress*, *J. Atm. Oceanic Technol.*, 26, 2, 368-382, [doi:10.1175/2008JTECHO578.1](https://doi.org/10.1175/2008JTECHO578.1), http://www.knmi.nl/publications/fulltexts/wind_stressjaotrev1.pdf

- Portabella, M. en A. Stoffelen, *A probabilistic approach for SeaWinds data assimilation*, Quart. J. Royal Meteor. Soc., 2004, **130**, 596, 127-159, [doi:10.1256/qj.02.205](https://doi.org/10.1256/qj.02.205), http://www.knmi.nl/publications/fulltexts/mss_paper_final_form.pdf
- Portabella, M. and A. Stoffelen (2002a), *A comparison of KNMI Quality Control and JPL Rain Flag for SeaWinds*, Canadian Journal of Remote Sensing, , 28, 3, 424-430.
- Portabella, M. and A. Stoffelen (2002b), *Characterization of Residual Information for SeaWinds Quality Control*, IEEE Transactions on Geoscience and Remote Sensing, , 40, 12, 2747-2759, [doi:10.1109/TGRS.2002.807750](https://doi.org/10.1109/TGRS.2002.807750).
- Portabella, M. and A. Stoffelen (2001), *Rain Detection and Quality Control of SeaWinds*, J. Atm. Oceanic Technol., , 18, 7, 1171-1183.
- Stoffelen, A. (2008), Research and Development in Europe on the Global Application of the OceanSat-II Scatterometer, *Announcement of Opportunity (AO) proposal submitted to ISRO on 30 June 2008*.
- Stoffelen, A., J. Vogelzang en A. Verhoef, *verification of scatterometer winds*, 10th International Winds Workshop, 20/2/2010-26/2/2010, M. Forsythe & J. Daniels (Ed), 2010, Tokyo, Japan, JMA, EUMETSAT. http://www.knmi.nl/publications/fulltexts/scat_iww10.pdf .
- Stoffelen, A. en M. Portabella, *On Bayesian Scatterometer Wind Inversion*, IEEE Transactions on Geoscience and Remote Sensing, 2006, **44**, 6, 1523-1533, [doi:10.1109/TGRS.2005.862502](https://doi.org/10.1109/TGRS.2005.862502). http://www.knmi.nl/publications/fulltexts/inversion_paper_ieee_final_form.pdf.
- Vogelzang, J., J. de Kloe, M. Portabella, A. Stoffelen, A. Verhoef and J. Verspeek (2010), SDP User Manual and Reference Guide version 2.1, *NWPSAF-KN-UD-002*, EUMETSAT
- Wikipedia, 2013, http://en.wikipedia.org/wiki/Earth_radius
- WMO OSCAR, 2013, <http://www.wmo-sat.info/oscar/>
- Yun, Risheng, Ad Stoffelen, Jeroen Verspeek, Anton Verhoef, Xiaolong Dong, NWP Ocean Calibration And Validation Of Ku-Band Scatterometers, IOVWST 2012, Utrecht, the Netherlands, 12-14 June 2012, http://coaps.fsu.edu/scatterometry/meeting/docs/2012_meeting/Posters_IOVWST/Yun_OCEAN_CALIBRATION_AND_VALIDATION_OF_KU-BAND_SCATTEROMETERS.pdf

The EUMETSAT
Network of
Satellite
Application
Facilities



OSI SAF

Ocean and Sea Ice

The EUMETSAT
Network of
Satellite
Application
Facilities



NWP SAF

Numerical Weather Prediction



Koninklijk Nederlands
Meteorologisch Instituut
Ministerie van Infrastructuur en Milieu